Pacific Northwest
NATIONAL LABORATORY

PNNL-30976, Rev. 0
RPT-DSA-001, Rev. 0

Maximum Cs-137 Curie Loading onto Crystalline Silicotitanate for the Documented Safety Analysis of the Tank Side Cesium Removal Platform

March 2021

SK Fiskum
EL Campbell
JL George
RA Peterson
TT Trang-Le

U.S. DEPARTMENT OF ENERGY

Prepared for the U.S. Department of Energy
under Contract DE-AC05-76RL01830

DISCLAIMER

PACIFIC NORTHWEST NATIONAL LABORATORY
operated by
BATTELLE
for the
UNITED STATES DEPARTMENT OF ENERGY
under Contract DE-AC05-76RL01830

Printed in the United States of America

Available to DOE and DOE contractors from the
Office of Scientific and Technical Information,
P.O. Box 62, Oak Ridge, TN 37831-0062;
ph: (865) 576-8401
fax: (865) 576-5728
email: reports@adonis.osti.gov

Available to the public from the National Technical Information Service
5301 Shawnee Rd., Alexandria, VA 22312
ph: (800) 553-NTIS (6847)
email: orders@ntis.gov <https://www.ntis.gov/about>
Online ordering: http://www.ntis.gov

PNNL-30976, Rev. 0
RPT-DSA-001, Rev. 0

Maximum Cs-137 Curie Loading onto Crystalline Silicotitanate for the Documented Safety Analysis of the Tank Side Cesium Removal Platform

March 2021

SK Fiskum
EL Campbell
JL George
RA Peterson
TT Trang-Le

Prepared for
the U.S. Department of Energy
under Contract DE-AC05-76RL01830

Pacific Northwest National Laboratory
Richland, Washington 99354

Summary

The Tank Side Cesium Removal (TSCR) system is currently being constructed to process Hanford tank waste supernates for vitrification. TSCR incorporates a filtration system and cesium (Cs) removal system using columns filled with crystalline silicotitanate (CST) ion exchanger, produced by Honeywell UOP, LLC. The documented safety analysis (DSA) developed for TSCR limits a single column curie loading to 141,600 Ci; given a ^{137}Cs isotopic mass fraction of 20% and the planned CST bed size of a TSCR column, this equates to 0.10 mmole Cs per g CST. Factors that influence ^{137}Cs loading onto the CST include, but are not limited to, CST production lot (different production lots behave differently), contact temperature, contact duration, ^{137}Cs mass fraction, and competitors in the tank waste feed. Seventeen tank waste feeds (compositions) were identified by Washington River Protection Solutions to potentially be processed through TSCR. In addition, Washington River Protection Solutions provided the supernate compositions of all the tanks in AP farm. However, the seventeen batches were found to have a wider composition range relative to those found in the AP tank farm; therefore, the initial planned seventeen batches were used for the evaluation. These feed compositions were used to develop a simulant (referred to herein as Stage 1) that would provide an upper bound to the Cs loading onto CST based on maximizing the Cs/Na activity coefficient ratios in solution while maintaining Na at no less than 5.0 M. Building upon this Stage 1 simulant, a series of four additional simulants were developed based on the cationic/anionic species that impact Cs exchange, with each successive formulation relaxing one or more matrix component concentration constraints as show in Table S.1

Table S.1 Simulant Formulations to Test the DSA

	Stage 1	Stage 2A	Stage 2B	Stage 3	AP-107
Ion	All ions at ±10% max/min	Low OH^-	High K^+	Low K^+, Low OH^-	Bounding first tank waste
			Molarity, As-Prepared		
Na^+	5.06	5.05	5.05	5.07	5.06
K^+	0.0450	0.0450	0.405	0.0720	0.0757
NO_3^-	1.22	1.37	1.50	1.25	1.60
F^-	0.0774	0.0773	0.0769	0.0774	0.0308
SO_4^{-2}	0.0770	0.0770	0.0769	0.0770	0.0627
OH^-	1.96	1.66	1.94	1.64	1.01
NO_2^-	0.334	0.554	0.491	0.659	0.944
CO_3^{-2}	0.682	0.638	0.649	0.682	0.714

The simulants were tested in a series of batch contacts with two separate production lots of CST. The most bounding Stage 1 simulant was contacted with CST at two temperatures (13 and 21 °C), where the time to reach equilibrium was found to be lower at 21 °C (96 h) than at 13 °C (240 h). CST lot 2002009604 reached equilibrium sooner than CST lot 2099000001. Isotherms were developed for the five simulant matrices and all resulted in higher loadings than can be accepted in the DSA for the initial feeds to TSCR; that is, Cs loading would be >0.10 mmole Cs per g CST at the Cs feed concentration of 6.8×10^{-5} M.

Two additional studies were conducted: 1) F-factor variability determined at two temperatures and 2) K_d measurement precision with the Baseline simulant.[1]

[1] Russell RL, PP Schonewill, and CA Burns. 2017. *Simulant Development for LAWPS Testing*. PNNL-26165, Rev. 0; RPT-LPIST-001, Rev. 0. Pacific Northwest National Laboratory, Richland, Washington.

1. The relative percent difference (RPD) was <2% in the duplicate pair F-factors when measured at both 105 °C and 427 °C. However, the 427 °C temperature basis was more precise (<0.61% RPD). Additionally, samples collected in three sets over a 3-week interval resulted in more precise F-factor values when heated to 427 °C. The F-factor value decreased ~6.6% when measured at 427 °C relative to measures at 105 °C. As the F-factor decreases, the Q (mmoles Cs per g dry CST) and Cs distribution coefficient (K_d) values increase.

2. Triplicate samples of CST lots 2002009604 and 2099000001 were contacted with the Baseline simulant (at ambient temperature) to assess overall K_d measurement precision. Using the ^{137}Cs tracer and gamma energy analysis measurement, relative standard deviations of 0.8% and 1.2% were achieved for CST lots 2002009604 and 2099000001, respectively.

Acknowledgements

The authors thank Dr. Gregg Lumetta for generating the Aqua Module in HSC Chemistry activity coefficients for Cs and K in various ionic strength solutions. We thank the Analytical Support Operations for simulant analysis. Specifically, we thank Dr. Samuel Morrison, Denis Cherkasov, and Jenn Carter for analysis by inductively coupled plasma mass spectrometry and inductively coupled plasma optical emission spectroscopy and subsequent data reviews. We thank Andrew Carney and Karl Pool for the analysis of free hydroxide and carbonate. We thank Jenn Carter for anion analysis by ion chromatography. We thank Renee Russell for conducting the technical review of numerous calculation files, test data packages, and this report. The authors also thank Bill Dey for the quality reviews of the calculation files and this report and Matt Wilburn for his technical editing contribution to this report.

Acronyms and Abbreviations

ASO	Analytical Support Operations
ASR	Analytical Service Request
CST	crystalline silicotitanate
DFLAW	Direct Feed Low-Activity Waste
DSA	documented safety analysis
EQL	estimated quantitation limit
ICP-MS	inductively coupled plasma mass spectrometry
ICP-OES	inductively coupled plasma optical emission spectroscopy
ILAW	immobilized low-activity waste
LAW	low-activity waste
MDL	method detection limit
PNNL	Pacific Northwest National Laboratory
QA	quality assurance
R&D	research and development
RPD	relative percent difference
RSD	relative standard deviation
TGA	thermogravimetric analysis
TSCR	Tank Side Cesium Removal
WRPS	Washington River Protection Solutions, LLC
WTP	Hanford Waste Treatment and Immobilization Plant
WWFTP	WRPS Waste Form Testing Program

Contents

Figures

Tables

1.0 Introduction

The initial production of immobilized low-activity waste (ILAW) is enabled by feeding tank waste supernate from the tank farms to the Tank Side Cesium Removal (TSCR) system and subsequent immobilization in the Hanford Waste Treatment and Immobilization Plant (WTP) Low-Activity Waste (LAW) Facility. Decanted tank waste supernatant will be pretreated using TSCR to meet the WTP LAW Facility waste acceptance criteria.[1] Within the TSCR system, cesium removal is planned to be accomplished using a non-elutable ion exchanger, crystalline silicotitanate (CST) produced by Honeywell UOP, LLC (Des Plaines, IL) under the product name IONSIV R9140-B.[2] Thus, ^{137}Cs will accumulate onto the CST columns with primary loading on the lead column (the first column in a sequential lead-lag-polish configuration). The TSCR CST media volume is 596 L (157.5 gal) loaded in an annular column with a bed height of 234 cm (92 inches) (Siewert 2019).

As part of the development of the TSCR documented safety analysis (DSA), a maximum ^{137}Cs column loading limit of 141,600 Ci (238 Ci ^{137}Cs/kg CST) has been established (Anderson 2020). Factors that influence the loading of ^{137}Cs onto the CST include, but are not limited to, CST production lot (different production lots behave differently), TSCR processing temperature, contact time with CST, ^{137}Cs isotopic mass fraction, matrix effects, and competitors in the tank waste feed. The total cesium loading limit onto CST can be estimated from the total column curie limit (presumably all curies are associated with ^{137}Cs), 20 wt% ^{137}Cs in the total cesium inventory, 596 L bed volume, and 1.0 kg/L CST bed density (Fiskum et al. 2019a). The cesium loading limit thus becomes 0.10 mole Cs/kg per Eq. (1.1).

$$\frac{141{,}600 \text{ Ci } ^{137}\text{Cs}}{(596 \text{ L CST}) \times \text{SpA} \times \text{MF} \times \text{FW} \times \rho} \tag{1.1}$$

where SpA = ^{137}Cs specific activity, 86.9 Ci/g
MF = ^{137}Cs isotopic mass fraction, 20%
FW = nominal Cs formula weight (representing tank waste Cs isotopic mass fractions), 134 g/mole
ρ = CST bed density, 1 kg/L

The expected conditions of the 17 Direct Feed Low-Activity Waste (DFLAW) tank waste batches expected to be processed by TSCR have been identified.[3] These batches were evaluated to assess the chemical bounding conditions maximizing Cs loading. In addition, Washington River Protection Solutions, LLC (WRPS) provided the supernate compositions of all the tanks in AP Farm. However, the seventeen batches were found to have a wider composition range relative to those found in the AP tank farm; therefore, the initial planned seventeen batches were used for the evaluation.

WRPS identified batch contact equilibrium test data as a basis to establish the minimum (or maximum) waste conditions necessary to prevent exceeding the ^{137}Cs column loading limit defined by the DSA. It

[1] 24590-WTP-ICD-MG-01-030, Rev. 0. 2015. *ICD 30 – Interface Control Document for Direct LAW Feed*. Bechtel National, Inc., Richland, Washington.
[2] CST is a Nb-substituted silicotitanate formulated by staff at Texas A&M University and Sandia National Laboratories and then manufactured in an engineered spherical form (Braun et al. 1996). Its chemical and physical properties, column dynamics, temperature tolerance, and radiation tolerance were previously described in a literature review (Pease et al. 2019).
[3] From KA Anderson to LH Cree. April 23, 2020. Interoffice Memorandum WRPS-2001428, "Anticipated Composition and Temperature Ranges for the First 10 Years of TSCR Operation"; Washington River Protection Solutions, Richland, Washington; not publicly available.

was hoped that these defined conditions could be used in establishing the TSCR waste acceptance criteria for the planned DFLAW campaigns.

The overall objective of this work was to develop equilibrium test data to establish the bounding waste matrix conditions necessary to prevent ^{137}Cs column loading limits from exceeding 0.10 moles Cs/kg CST for a range of total Cs (^{137}Cs), Na, and K concentrations. These conditions could then be used in establishing the TSCR waste acceptance criteria for the planned DFLAW campaigns. In support of this overall objective, the specific objectives of this testing were defined in three tasks as follows.

Task 1: Define the simulant matrix conditions to be used in the equilibrium testing with explanation as to how this bounds the feed conditions for the various DFLAW campaigns.

Task 2: Perform equilibrium testing using the simulant conditions determined in Task 1.

a. Define the F-factor[1] at two drying temperatures, 100 °C and 427 °C, to help determine the optimum approach to establish the dry mass of CST.
b. Determine Cs uptake after 48, 96, 168, and 240 h (unless equilibrium can be demonstrated in less time) to establish an appropriate contact time for equilibrium Cs exchange.
c. Perform isotherm testing using the simulant conditions determined in Task 1 to demonstrate Cs loading capacity at the feed condition.

Task 3: Establish the Baseline simulant (Russell et al. 2017) Cs distribution coefficient (K_d) precision metric from equilibrium contact testing in triplicate.

Two different lots of CST were provided by WRPS for this investigation: lot 2002009604 and lot 2099000001.

[1] The F-factor corrects for water content in the CST. It is calculated from the mass of dry CST divided by the mass of the as-sampled, undried CST.

2.0 Quality Assurance

All research and development (R&D) work at Pacific Northwest National Laboratory (PNNL) is performed in accordance with PNNL's Laboratory-Level Quality Management Program, which is based on a graded application of NQA-1-2000, *Quality Assurance Requirements for Nuclear Facility Applications* (ASME 2000), to R&D activities. To ensure that all client quality assurance (QA) expectations were addressed, the QA controls of the PNNL's WRPS Waste Form Testing Program (WWFTP) QA program were also implemented for this work. The WWFTP QA program implements the requirements of NQA-1-2008, *Quality Assurance Requirements for Nuclear Facility Applications* (ASME 2008), and NQA-1a-2009, *Addenda to ASME NQA-1-2008* (ASME 2009), and consists of the WWFTP Quality Assurance Plan (QA-WWFTP-001) and associated QA-NSLW-numbered procedures that provide detailed instructions for implementing NQA-1 requirements for R&D work.

The work described in this report was assigned the technology level "Applied Research" and was planned, performed, documented, and reported in accordance with procedure QA-NSLW-1102, *Scientific Investigation for Applied Research*. All staff members contributing to the work received proper technical and QA training prior to performing quality-affecting work.

3.0 Simulant Formulation and Preparation

This section describes the approach to simulant formulations with the objective of maximizing Cs loading onto CST. Simulant preparation and analysis is also described. All work was conducted according to a test plan prepared by PNNL staff and approved by WRPS.[1]

3.1 Simulant Formulations for the DSA

WRPS provided to PNNL a suite of feed compositions expected to represent the first 17 tank waste batches processed through TSCR (DFLAW campaigns). The feed compositions were based on the Best Basis Inventory of Hanford tank waste and TOPSim[2] modeling predictions; components were limited to those present at >0.01 M and Cs (see Table 3.1).

[1] Fiskum SK. 2020. TP-DFTP-101, Rev. 1.0. *TSCR Documented Safety Analysis Ion Exchange Media Equilibrium Batch Contacts (Max Currie Loading)*. Pacific Northwest National Laboratory, Richland Washington. Not publicly available.

[2] TOPSim modeling has been previously described by Bernards et al. (2018).

Table 3.1. Simulant Composition Basis for the First 17 DFLAW Processing Campaigns, Normalized to 5 M Na

	DFLAW Campaign																				
	1	2	3	4	5	6	7	8	9	10	11	12	13	14	15	*16*	*17*	Min.	Max.	Avg.	
	Simulant Test Stage																				
	3	3	3	3	3	3	2A	3	2B	3	3	3	3	3	2A	(a)	(a)				
Species	Molarity																				
$Al(OH)_4^-$	0.12	0.15	0.12	0.12	0.13	0.16	0.17	0.16	0.19	0.14	0.12	0.14	0.14	0.14	0.13	*0.07*	*0.05*	0.12	0.19	0.14	NA
$C_2O_4^{-2}$	0.01	0.01	0.01	0.01	0.01	0.01	0.01	0.01	0.01	0.01	0.01	0.01	0.01	0.01	0.01	*0.01*	*0.01*	0.01	0.01	0.01	NA
Cl^-	0.09	0.10	0.09	0.09	0.09	0.09	0.06	0.06	0.05	0.07	0.08	0.08	0.08	0.08	0.08	*0.04*	*0.02*	0.05	0.10	0.08	Min
CO_3^{-2}	0.57	0.40	0.48	0.49	0.48	0.44	0.58	0.59	0.59	0.59	0.62	0.52	0.52	0.52	0.48	*0.24*	*0.18*	0.40	0.62	0.52	Max
CrO_4^{-2}	0.01	0.01	0.01	0.01	0.01	0.01	0.01	0.01	0.01	0.01	0.01	0.01	0.01	0.01	0.01	*0*	*0*	0.01	0.01	0.01	NA
Cs^+ ($\times 10^{-5}$)	6.73	5.60	6.84	6.71	5.53	4.85	4.75	4.44	4.39	5.59	4.74	5.46	4.99	4.79	3.98	*1.75*	*0.884*	4.0	6.8	5.29	
F^-	0.03	0.01	0.01	0.01	0.01	0.01	0.04	0.03	0.07	0.04	0.02	0.03	0.02	0.02	0.01	*0.01*	*0.01*	0.01	0.07	0.02	Max
K^+	0.08	0.12	0.09	0.09	0.11	0.10	0.05	0.08	0.45	0.25	0.11	0.15	0.11	0.09	0.06	*0.02*	*0.01*	0.05	0.45	0.13	
Na^+	5.83	5.55	5.52	5.52	5.52	5.51	5.89	5.61	5.53	5.5	5.5	5.51	5.51	5.51	5.5	*5.5*	*5.5*	5.50	5.89	5.57	
NO_2^-	1.19	1.22	1.12	1.11	1.12	1.18	0.98	0.96	0.93	1.05	1.09	1.11	1.13	1.13	0.99	*0.99*	*1.01*	0.93	1.22	1.09	Min
NO_3^-	1.96	1.86	2.34	2.3	1.91	1.83	1.47	1.31	1.61	1.77	1.53	1.69	1.68	1.61	1.68	*2.78*	*3.29*	1.31	2.34	1.77	Min
OH^- (free)	1.05	1.43	1.12	1.12	1.26	1.49	1.51	1.4	1.76	1.32	1.15	1.34	1.34	1.3	1.17	*0.66*	*0.48*	1.05	1.76	1.32	Max
PO_4^{-3}	0.02	0.01	0.02	0.02	0.02	0.02	0.02	0.03	0.02	0.02	0.03	0.02	0.02	0.02	0.04	*0.04*	*0.04*	0.01	0.04	0.02	Min
SO_4^{-2}	0.06	0.03	0.05	0.05	0.04	0.04	0.06	0.06	0.05	0.04	0.07	0.04	0.05	0.05	0.05	*0.04*	*0.03*	0.03	0.07	0.05	Max
TOC	0.15	0.23	0.16	0.16	0.17	0.14	0.11	0.11	0.13	0.14	0.13	0.14	0.14	0.14	0.13	*0.06*	*0.03*	0.11	0.23	0.15	NA

Tank Waste Compositions (M) for first 17 DFLAW Processing Campaigns, normalized to 5 M Na (from WRPS Interoffice Memorandum, WRPS-2001428, dated April 23, 2020 to LH Cree from KA Anderson, Table 5, TOPSim Prediction for CaseID: 6858)

(a) Campaigns 16 and 17 were omitted from the evaluation because of the low cesium and potassium concentrations.
Notes:

- Green shading: maximum and minimum values of selected components.
- Blue shading: concentrations that do not pass Stage 3 limits.
- Boxed values: concentrations that represent the minimum or maximum values in the row of selected analytes.

Theoretical understanding of the Cs loading (Zheng et al. 1997) indicates that maximizing the Cs-to-Na activity coefficient ratio will result in maximum Cs loading. Pursuant to this approach, activity coefficients for the various components in the feed solutions were calculated using the Aqua Module in HSC Chemistry version 7.193 (Outotec Research Center). The Harvie formalism was applied in the calculation of the activity coefficients. Charge balance between anions and cations in the projected feed solutions was adjusted by changing the nitrate concentration as needed to result in complete electrical neutrality for the start of each scan. Each anion was then increased through the addition of the sodium salt of that anion. Calculations were conducted for a temperature of 25 °C. Additional calculations demonstrated that changing temperature had limited impact on the ratio of activity coefficients. Table 3.2 provides the baseline composition (from the limiting compositions in Table 3.1 normalized to 5 M Na) for the calculations. Individual components were varied over the anticipated range of compositions from this baseline composition.

Table 3.2. Baseline Composition for Activity Coefficient Calculations

Species	mole/L	Range, M
H_2O	53.6	
Na^+	5.00	constant
K^+	0.0400	constant
Cs^+	0.0001	constant
NO_3^-	0.431	0.43 – 3.13
OH^-	1.74	0.43 – 1.93
NO_2^-	1.21	0.84 – 1.24
AlO_2^-	0.119	0.045 – 0.195
CO_3^{2-}	0.613	0.16 – 0.66
SO_4^{2-}	0.0690	0.027 – 0.075
Cl^-	0.0160	0.016 – 0.103
F^-	0.0080	0.008 – 0.068
PO_4^{3-}	0.0400	0.009 – 0.041
$C_2O_4^{2-}$	0.0090	constant
CrO_4^{2-}	0.0080	0.001 – 0.011

The HSC software allows specific components to be varied over a range of concentrations. These calculations were performed for aluminate, hydroxide, nitrate, nitrite, phosphate, sulfate, chloride, carbonate, chromate, and fluoride. These anions were specifically evaluated because they dominate the tank waste anionic composition. The ratio of the Cs/Na activity coefficients and the ratio of the K/Na activity coefficients can then be calculated. Figure 3.1 and Figure 3.2 show the impact of each anion (split into two sets) on the Cs/Na activity coefficient ratios. It should be noted that both the anion and Na concentrations are changing at the same time, so what is shown is the effective impact of the anion, as all anions have an inherent sodium impact imbedded.

Note that Figure 3.1 indicates that carbonate should inhibit cesium loading. However, an assessment of the Bromley coefficients indicated that the Bromley coefficient for cesium carbonate would be higher than that for sodium carbonate, indicating that carbonate would have the effect of enhancing cesium loading (Bromley 1973). Fondeur et al. (2000) also observed enhanced Cs uptake with increasing carbonate concentration. To resolve this discrepancy, tests of a simple simulant matrix with carbonate, nitrate, and hydroxide were performed. These tests confirmed that carbonate enhanced cesium loading under these conditions.

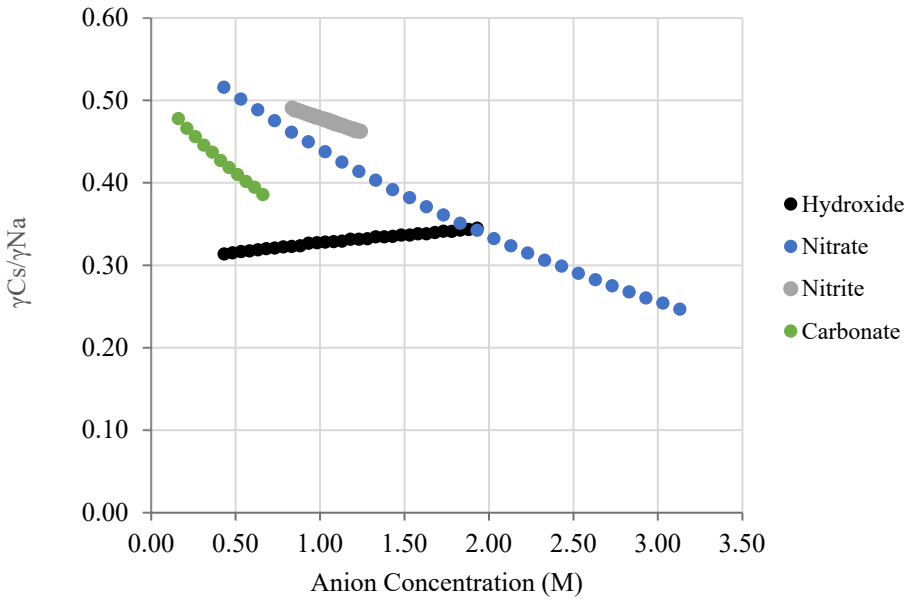

Figure 3.1. Cs/Na Activity Coefficient vs. Anion Set 1 Molar Concentrations

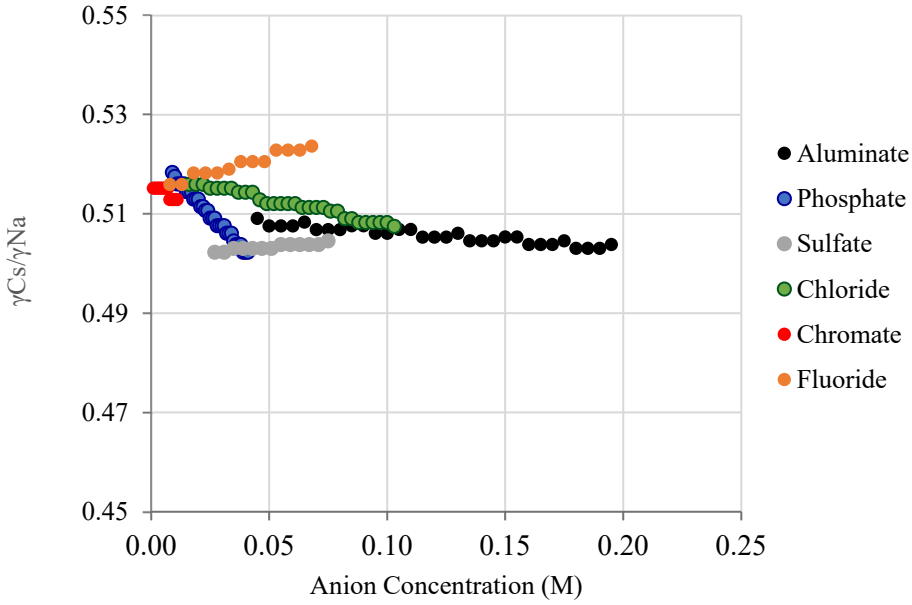

Figure 3.2. Cs/Na Activity Coefficient vs. Anion Set 2 Molar Concentrations

Table 3.3 provides a summary of the impact of the various cations and anions on loading behavior as well as the anions that were selected to develop the test simulants. The minor anions that inhibit Cs exchange or have no significant impact on Cs exchange were omitted from further consideration. (Note that the last two batches, #16 and #17, were omitted from this evaluation as they have very low projected cesium concentrations, but also very low potassium concentrations that, if included, would likely cause the test to fail the cesium loading limit. These batches are expected to be assessed later.) Remaining components were set to their minimum (for inhibitors) or maximum (for favoring) values, with an added 10% constraint based on Table 3.1 values. This 10% constraint bounded the potential analysis uncertainty.

However, the resulting simulant formulation was not charge-balanced. Therefore, the nitrite concentration was adjusted to charge-balance the simulant composition. All simulant Na concentrations were targeted to 5.0 M; lower Na concentrations result in higher Cs loading (Brown et al. 1996). The target Na concentration for processing is 5.6 M and the 5.0 M Na target concentration encompassed a 10% measurement uncertainty..

Table 3.3. Cation and Anion Impact on Cs Loading and Selection for Simulant

Component	Influence of Cs loading on CST	Target, Normalized to 5 M Na
$Al(OH)_4^-$	No significant impact	Not included
$C_2O_4^{-2}$	No significant impact	Not included
Cl^-	Inhibits	Not included
CO_3^{-2}	Favors	Maximum + 10%
CrO_4^{-2}	No significant impact	Not included
F^-	Favors	Maximum + 10%
K^+	Inhibits	Minimum – 10%
Na^+	Inhibits	Normalized to 5 M
NO_2^-	Inhibits	Used to balance anions
NO_3^-	Inhibits	Minimum – 10%
OH^-	Favors	Maximum + 10%
PO_4^{-3}	Inhibits	Not included
SO_4^{-2}	Favors	Maximum + 10%

The simplest approach was to bound all DFLAW campaigns (1-15) by setting the selected component concentrations to the appropriate maximum or minimum values (green shaded blocks in Table 3.1) with the added 10% contingency. This is represented as Stage 1 simulant in the Table 3.1 sub-header. If the Cs loading limit for Stage 1 simulant passed the criterion, then all DFLAW campaigns would pass the criterion.

There was a reasonable probability that the cesium loading limit for the Stage 1 simulant would be too high. Thus, Stage 2 of testing relaxed the limits for selected components, in particular, potassium and hydroxide, as these are known to impact cesium loading. Inspection of Table 3.1 shows that batches 7, 9, and 15 are characterized by low cesium concentrations concomitant with either high hydroxide or low potassium concentrations. Therefore, two simulants, Stages 2A and 2B, were formulated to bound the low hydroxide and high potassium concentrations, respectively.

Finally, Stage 3 testing relaxed the potassium and hydroxide constraints by removing batches 7, 9, and 15 from the limiting conditions. Thus, the minimum potassium concentration is higher than those of Stage 1 and Stage 2A and the maximum hydroxide concentration is lower than those of Stage 1 and Stage 2B.

Table 3.1 lists at the top, the last stage at which a given DFLAW campaign could pass the criteria. All campaigns are within the Stage 1 limits. Those listed as Stage 2A or Stage 2B only pass with the respective simulant limits from those tests (but not Stage 3). Stage 3 feeds pass all DFLAW campaigns except campaigns 7, 9, and 15. The target compositions for these simulants are further discussed in Section 4.0.

3.2 AP-107 Simulant Formulation for the DSA

Based on preliminary equilibrium testing results from the Baseline and Stage 1 simulants, it was identified that cesium concentration in solution would likely exceed the target Cs loading onto CST for all simulant stages. Therefore, an additional round of testing was added to the scope to directly identify the bounding loading that could be achieved with AP-107. An AP-107 simulant was formulated based on

previously measured constituent values for AP-107 tank waste (Fiskum et al. 2019a; Rovira et al. 2018). The constituents that inhibit cesium loading were reduced in concentration by 10%. The constituents that increase cesium loading were increased in concentration by 10%. The target composition for this simulant is further discussed in Section 3.4.

3.3 Baseline Simulant Formulation

The Baseline simulant was formulated as previously described (Russell et al. 2017). However, sodium oxalate was omitted from the formulation to mitigate solids precipitation. Further, the Cs concentration was revised from 1.04×10^{-4} M (13.8 µg/mL) to 5.0×10^{-4} M (66.3 µg/mL). This modified Cs concentration was specified in the WRPS statement of work and provided a more measurable basis by inductively coupled plasma mass spectrometry (ICP-MS), as used by Honeywell UOP, LLC supporting production testing.

3.4 Simulant Preparation

All simulants were prepared from American Chemical Society reagent grade materials shown in Table 3.4 and according to a test instruction.[1] Component masses were measured into volumetric flasks containing part of the requisite deionized water. Table 3.5 show the added salt quantities and order of addition. The addition of Na_2CO_3 was conducted while swirling the volumetric flask to the extent practical; however, in most cases, some of the Na_2CO_3 appeared to agglomerate as a clump. The Na_2CO_3 agglomerate dissolved slowly, taking generally ~12 to 24 h to complete dissolution. When the solution was mixed, some gas evolution was noted. Thus, the extent that carbonate remained in solution versus expulsion as CO_2 from a saturated solution was not clear; analysis was required to define final concentration of the dissolved carbonate. After all salts were added and dissolved, the solution was brought to volume with deionized water.

Table 3.4. Reagents Used for Simulant Production

Compound	MW, g/mole	Manufacturer	Product Number	Lot Number	Assay, %
$Al(NO_3)_3\cdot9H_2O$	375.1	Sigma-Aldrich	237973-500g	BCBR0256V	99.9
Na_2CO_3	105.99	Sigma Aldrich	222321-500g	MKCM9200	99.54
NaF	41.99	Sigma Aldrich	201154-100g	MKCM8713	100.2
KNO_3	101.1	Fisher	P263-500	155173	99.9
$NaNO_2$	69.00	Sigma-Aldrich	237213-2.5kg	MKBV1410V	100.1
$NaNO_3$	85.00	Alpha Aesar	14493	Q16F033	99.60
$Na_3PO_4\cdot12H_2O$	380.1	Fisher	S377-500	126469	100.8
Na_2SO_4	142.0	Sigma-Aldrich	239313-500g	SLBN9500V	99.7
50% NaOH	40.00	Sigma Aldrich	72064-500	BCBZ4353	50.0
$CsNO_3$	194.9	Johnson and Matthey	14440	015016	99.99
KCl	74.6	Sigma-Aldrich	746436-500G	SLBR9127V	99.9

[1] Fiskum SK. 2020. TI-DFTP-102, *Simulant Preparation for DSA Study*. Pacific Northwest National Laboratory, Richland, Washington. Not publicly available. Implemented October-November 2020.

Table 3.5. Component Masses for Stage 1, 2A, 2B, 3, and AP-107 Simulant Preparations

Compound	Stage 1 Simulant, g / 2.0 L	Stage 2A Simulant, g / 0.25 L	Stage 2B Simulant, g / 0.25 L	Stage 3 Simulant, g / 0.25 L	AP-107 Simulant, g / 0.25 L
Water	1697	212.6	207.8	212.4	214.8
KNO_3	9.1084	1.1382	10.2461	1.8218	1.9156
$NaNO_3$	201.2189	28.2290	23.2601	25.1421	32.5259
NaF	6.4894	0.8101	0.8054	0.8111	0.3228
Na_2SO_4	21.9386	2.7432	2.7407	2.7416	2.2317
50% NaOH	312.7573	33.2353	38.7294	32.7190	20.1351
$NaNO_2$	46.0971	9.5458	8.4625	11.3590	16.2650
Na_2CO_3	145.3040	16.9911	17.2841	18.1441	19.0142
Density, g/mL	1.220	1.221	1.237	1.221	1.229

All densities were measured in the preparation volumetric flask at room temperature, ~20 °C (see Table 3.5). Each solution was passed through a 0.45-micron pore size nylon filter. The densities were remeasured and agreed with the pre-filtered solution density within expected uncertainty.

Table 3.6 provides the calculated component concentrations for the Stage 1, 2A, 2B, 3, and AP-107 simulants. A sample of each simulant was submitted to the PNNL Analytical Support Operations (ASO) laboratory under Analytical Service Request (ASR) 1177 for anion analysis by ion chromatography (F^-, Cl^-, NO_3^-, NO_2^-, PO_4^{3-}, and SO_4^{2-}); Al, Na, K, S, and P analysis by inductively coupled plasma optical emission spectroscopy (ICP-OES); Cs analysis by ICP-MS; free hydroxide analysis using potentiometric acid titration; and carbonate analysis by acid-catalyzed furnace oxidation.

Table 3.7 provides the measured analyte concentrations. Bracketed results were less than (<) the estimated quantitation limit (EQL) but greater than or equal to (≥) the method detection limit (MDL) and were reported as qualitative. For concentrations measured > EQL, the analysis results agreed with the calculated (as-prepared) concentrations within ±10% except three nitrate values, one hydroxide value, and one carbonate value, which were 10% to 13% high. The calculated concentrations for all components except carbonate were considered definitive. Because loss of carbonate was possible during simulant preparation, the measured concentration was expected to be the definitive value. The Cs was measured in these simulants to assess if Cs impurity in reagent salts was relevant. The highest measured concentration of 1.56×10^{-7} M Cs represented 0.057% of the lowest Cs spike concentration (2.76×10^{-4} M) in the isotherm study, and thus was considered irrelevant.

Table 3.6. Stage 1, 2A, 2B, 3, and AP-107 Simulants Calculated Compositions

Simulant>>	Stage 1	Stage 2A	Stage 2B	Stage 3	AP-107
Matrix notes>>	All ions at ±10% max/min	Low OH^-	High K^+	Low K^+ low OH^-	Bounding first tank waste
Ion	Calculated Molarity				
Na^+	5.06	5.05	5.05	5.07	5.06
K^+	0.0450	0.0450	0.405	0.0720	0.0757
NO_3^-	1.224	1.368	1.495	1.250	1.600
F^-	0.0774	0.0773	0.0769	0.0774	0.0308
SO_4^{-2}	0.0770	0.0770	0.0769	0.0770	0.0627
OH^-	1.96	1.66	1.94	1.64	1.01
NO_2^-	0.334	0.554	0.491	0.659	0.944
CO_3^{-2}	0.682	0.638	0.649	0.682	0.714

Table 3.7. Measured Stage 1, 2A, 2B, 3, and AP-107 Simulant Compositions (ASR 1177)

	Stage 1 Simulant	Stage 2A Simulant	Stage 2B Simulant	Stage 3 Simulant	AP-107 Simulant
Ion	Measured Molarity				
Na^+	4.96	4.87	4.65	4.92	5.00
K^+	0.0476	0.0481	0.427	0.0778	0.0803
Cs^+	<5.3E-09	1.55E-07	<5.3E-09	1.56E-07	[1.0E-06]
NO_3^-	1.37	1.49	1.66	1.41	1.71
F^-	[0.10]	[0.10]	[0.095]	[0.10]	[0.053]
SO_4^{-2}	[0.082]	[0.078]	[0.079]	[0.081]	[0.062]
OH^-	2.08	1.88	2.05	1.79	1.08
NO_2^-	0.352	0.576	0.515	0.713	0.989
CO_3^{-2}	0.661	0.634	0.700	0.735	0.792

Precision and bias are reported by the ASO to be ±15% or better for non-complex aqueous samples that are free of interference. Bracketed value indicates qualitative result; result is ≥ MDL but < EQL. The Al, P, Cl^-, and PO_4^{3-} results were < MDL.

Table 3.8 provides the measured component masses used in preparation of the Baseline simulant. A sample of the Baseline simulant was submitted to the ASO per ASR 1177 and analyzed in parallel with the other prepared simulants. The calculated matrix concentrations are shown in Table 3.8 adjacent to the measured matrix concentrations. For concentrations measured at >EQL, the analysis results agreed with the calculated (as-prepared) concentrations within ±10% except nitrate, which was 11% high, and hydroxide which was 15% high.

Table 3.8. Baseline Simulant Preparation and Composition

Compound	Measured, g / 1.0 L	Ion	Prepared, M	Measured, M
Water	757.8			(ASR 1177)
$Al(NO_3)_3 \cdot 9H_2O$	62.2531	Al as $Al(OH)_4^-$	0.166	0.158
KCl	9.1034	K^+	0.122	0.128
--	--	Cl^-	0.122	[0.14]
$Na_3PO_4 \cdot 12H_2O$	16.4185	PO_4^{3-}	0.043	[0.052]
$NaNO_3$	108.9600	NO_3^-	1.77	1.97
Na_2SO_4	9.3899	SO_4^{2-}	0.066	[0.068]
50% NaOH	165.9281	free OH^-	1.411	1.62
$NaNO_2$	70.3664	NO_2^-	1.020	1.106
Na_2CO_3	49.5000	CO_3^{2-}	0.465	0.532
$CsNO_3$	0.0972	Cs^+	4.99E-04	4.71E-04
--	--	Na^+	5.562	5.22
Density, g/mL	1.250			

Precision and bias are reported by the ASO to be ±15% or better for non-complex aqueous samples that are free of interference. Bracketed value indicates qualitative result; result is ≥ MDL but < EQL.
F^- was <MDL.

4.0 Experimental

This section describes the CST, F-factor determination, experimental conditions to conduct batch contact testing to assess 1) time to equilibrium, 2) isotherms, and 3) distribution coefficient (K_d) measurement precision.

4.1 CST

WRPS provided two lots of CST manufactured by Honeywell UOP, LLC as IONSIV™ R9140-B, 18 × 50 mesh, for testing. PNNL received a sample from CST lot[1] number 2002009604 on September 20, 2018, from WRPS. Delivery and initial subsampling were described previously (Fiskum et al. 2019b). PNNL received a sample from CST lot number 2099000001 on October 21, 2020, as directed by WRPS, from AVANTech (Richland, Washington). This sample was collected from the top of a 50-gallon drum by AVANTech staff.

The CST was used as-received. The CST materials were not sieved to produce a smaller CST size fraction and no pretreatment washing was applied. The assessment of the F-factor precision and repeatability was thought best to be compared on the material as-received, not confounded with damp material likely to continue drying with extended shelf time. The batch contact tests used a high liquid volume to CST mass ratio. Any colloidal fines associated with the CST rinsing would minimally impact the contact solution. Colloidoil mass loss was deemed an insignifcant factor and would not seriously bias the measured CST mass.

CST subsamples from each lot were collected into small jars in sufficient mass to support the test matrix. This eased overall subsampling efforts. Before subsampling, the contents were mixed by hand tumbling.

4.2 F-Factor

The F-factor (dry mass per sampled mass) was determined after heating CST at two temperatures: 105 °C and 427 °C. Because the CST was not pretreated by rinsing, the F-factor was expected to be relatively high and stable from one sampling event to the next. The F-factor was determined in duplicate each time CST was sampled for an experiment.

A measured mass (~0.3 to 0.5 g) of CST was placed into a tared glass vial. The vial was placed into an Isotemp vacuum oven (Fisher Scientific Model 280A) set to 105 °C. The vial was periodically removed from the oven and allowed to cool until the glass threads were cool to the touch, but the main vial body was still warm. Then the vial was capped, cooled completely, and the gross mass measured. The net mass of CST was determined. Typically, mass measures were collected every 7 to 12 h (a 70-h interval bridged a weekend) until the mass change was <0.5% between successive drying-weighing events.

Similarly, a measured mass of CST was placed into a tared stainless-steel crucible. The crucible was placed into a Thermoline furnace (Fisher Scientific Model FB1415) that was preheated to 427 °C. After 4 h, the crucible was removed from the furnace and placed into a desiccator containing moisture-indicating Drierite desiccant to cool. Then the gross mass was measured. The 4-h time at 427 °C was considered sufficient to completely remove all water from the CST matrix. (This was confirmed by the thermogravimetric analysis [TGA] isothermal hold at 427 °C where no significant additional weight loss was measured.)

[1] Honeywell UOP interchanges terms “lot number” and “batch number.”

4.3 Thermogravimetric Analysis

Thermogravimetric analysis (TGA) was performed using a TA Instruments Q600 DSC unit (New Castle, Delaware). Both lots of CST media were tested in duplicate and for all measurements, 30 mg (±1 mg) of sample was placed in an alumina flat-bottom crucible, and the temperature program was executed under air flowing at 50 mL/min. Samples were heated from room temperature to 100 °C at 5 °C/min, held for 1 h at 100 °C, then heated to 427 °C at 5 °C/min, held for 1 h at 427 °C, then heated at 5 °C/min to 600 °C.

4.4 Time to Equilibrium Cs Exchange Testing

The Cs uptake as a function of time was assessed to establish the contact time required to reach equilibrium Cs distribution condition. Both CST lots were tested with the Stage 1 simulant at 13 °C and 21 °C and with the Baseline simulant at 21 °C.

A 908.1-mL aliquot of the Stage 1 simulant was spiked with 0.672 mL of 0.753 M $CsNO_3$ solution to attain 5.57×10^{-4} M Cs. A 500-mL aliquot of the Baseline simulant was used as-prepared with 4.99×10^{-4} M Cs. All solution transfers were measured by mass; volumes were calculated after density corrections. Each stock solution was spiked with ^{137}Cs tracer, 0.277 μCi/mL for the Stage 1 simulant and 0.245 μCi/mL for the Baseline simulant. The additional total Cs mass from the tracer was <<1% of the spiked $CsNO_3$ solution component. Duplicate 2-mL subsamples were collected as reference ^{137}Cs concentrations (A_0).

Nominal 1.18-g aliquots of CST were measured into 250-mL poly bottles (actual masses measured to nearest 0.0001 g). The CST masses were corrected per the F-factor mass measured at 105 °C. A nominal 208-mL of traced simulant was added to each bottle containing CST; actual volume transferred was determined from the net mass corrected for density. See Appendix A for specific CST masses and simulant volumes. The contact solutions for testing at 13 °C were pre-chilled before adding to the CST. The initial liquid volume to solids mass phase ratio was ~202. The ~42-mL headspace in this configuration allowed for significant fluid motion, assuring good mixing.

A Benchmark (Sayreville New Jersey) Incu-Shaker™ 10LR refrigerated orbital shaker with 19-mm orbit, set to 200 rpm, was used for testing at the target 13 °C temperature. A Cole-Parmer (Vernon Hills, Illinois) large orbital shaker with a 16-mm orbit, set to 240 rpm, was used for testing at room temperature, nominally 21 °C. The shaking parameters were sufficient to lift the CST off the vessel floor but did not disperse the CST throughout the fluid volume. Temperature was periodically measured on a “sentinel” containing 220 mL of water in a 250-mL bottle, consistent with the sample geometry. The sentinel was removed from the shaker and water temperature measured with a Type K thermocouple (measurement uncertainty of ± 2.2 °C). The temperatures during contact remained relatively constant as shown in Figure 4.1. Dashed horizontal lines mark the upper and lower bounds of the measurement tolerance established in the test plan. The error bars represent the individual measurement uncertainty.

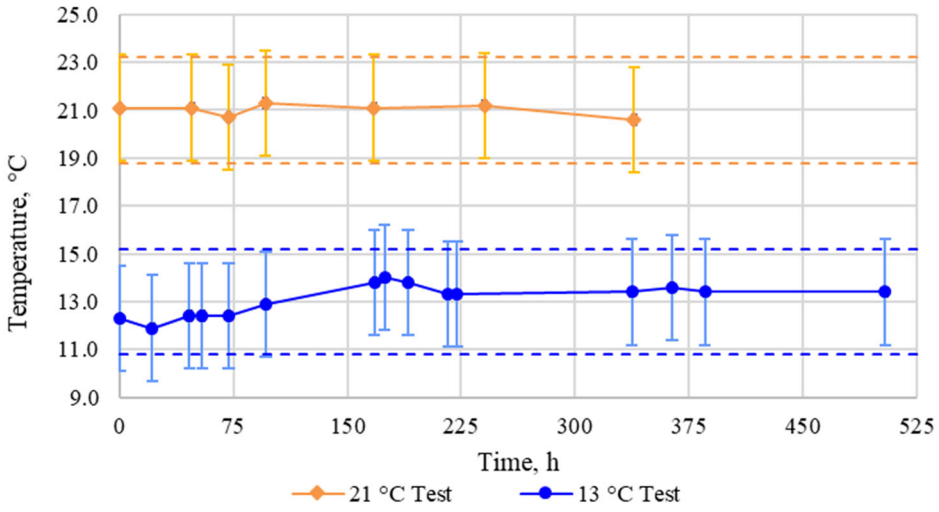

Figure 4.1. Temperature Profiles during Equilibrium Testing, 13 °C and 21 °C

Sampling occurred after nominally 48, 72, 96, 168, 240, and 338 h contact times; the chilled sample tests continued to a final sampling time of 504 h. The test duration extended beyond the test plan defined limit of 240 h because the equilibrium was not ascertained by 240 h. Two-milliliter sample aliquots were collected at each sample interval and passed through a 0.45-micron pore size nylon syringe filter before analysis. The volume change in the parent bottle was determined from the measured net solution mass and accounted for in the distribution coefficient (K_d, mL/g) and metal loading onto CST (Q, mmoles metal per g CST) calculations. A 2-mL volume-reduction during kinetic testing sampling represented ~0.9% of the total solution volume. After seven samplings, the contact solution volume reduction was ~6%.

Cs uptake was measured from the ^{137}Cs concentrations in the uncontacted stock solution and the aliquots collected, as a function of time, from the sample supernate. The tracer allowed for accurate ^{137}Cs determination, which can be related directly to total Cs uptake.

4.5 Isotherm Testing

Isotherm testing was split into two phases. The first phase evaluated both CST lots, 2002009604 and 2099000001, to determine which lot had the higher Cs exchange capacity at the nominal feed condition of 6.8×10^{-5} M Cs in Stage 1 simulant. The second phase only tested CST lot 2002009604 with the remaining four simulants (Stages 2A, 2B, 3, and AP-107). Note that 6.84×10^{-5} M Cs is the highest Cs concentration identified for the initial 17 batches of feed to TSCR.

A series of test solution concentrations were prepared such that the post-contacted equilibrium Cs concentrations would bracket the target 6.8×10^{-5} M Cs. A 250-mL aliquot of the Stage 1 simulant was spiked first with ^{137}Cs tracer. Duplicate 2-mL subsamples were collected as reference ^{137}Cs concentrations (A_0). Various aliquots of $CsNO_3$ solutions were transferred to each of four 60-mL polyethylene bottles. Then 60-mL of traced Stage 1 simulant was transferred to each of the bottles. The Cs mass from the tracer was <<1% of the added stable Cs component. The traced simulant samples combined with the $CsNO_3$ solution were allowed to equilibrate overnight. Stage 2A, 2B, 3, and AP-107 simulants were similarly prepared with ^{137}Cs tracer and $CsNO_3$ solutions, albeit with smaller stock volumes of 150 mL each and subaliquots of 30 mL each. See Appendix B for specific CST masses and simulant volumes. As with the equilibrium test sample set, all solution transfers were measured by mass; volumes were calculated after

density corrections. Table 4.1 provides the calculated initial Cs concentrations of the individual batch contact stock samples. Note that although the simulants are identified as "stages," all testing was conducted concurrently to reduce overall schedule.

Table 4.1. Simulant Cs Concentrations in the Isotherm Test Solutions

Sequence ID	Stage 1	Stage 2A	Stage 2B	Stage 3	AP-107
	Cs Molarity				
1	2.76E-4	2.84E-4	2.85E-4	2.90E-4	2.90E-4
2	5.56E-4	5.78E-4	5.69E-4	5.85E-4	5.67E-4
3	1.24E-3	1.27E-3	1.25E-3	1.28E-3	1.31E-3
4	1.23E-2	1.24E-2	1.23E-2	1.28E-2	1.24E-2

Nominal 0.075-g (dry mass basis) aliquots of CST were measured into 20-mL polyethylene vials (actual masses measured to nearest 0.0001 g). The CST masses were corrected per the F-factor mass measured at 105 °C. A nominal 15 mL of traced simulant was added to each vial containing CST; actual volume transferred was determined from the net mass corrected for density. See Appendix B for specific CST masses and simulant volumes. The liquid volume to solids mass phase ratio was ~202. The ~5-mL headspace in this configuration allowed for significant fluid motion, assuring good mixing. Stage 1 simulant samples were mixed for 288 h and Stage 2A, 2B, 3, and AP-107 simulant samples were mixed for 238 h. All mixing was conducted in the Benchmark Incu-Shaker™ 10LR refrigerated orbital shaker at 13 °C. After processing, a nominal 2-mL sample aliquot was filtered through a 0.45-micron pore size nylon syringe filter and the filtrate was collected for ^{137}Cs analysis.

4.6 Baseline Simulant Equilibrium Precision Test

Equilibrium batch contact testing was conducted in triplicate on both CST lots, 2002009604 and 2099000001, to develop precision assessments. Testing was conducted much as previously described for isotherm testing. A 100-mL aliquot of the Baseline simulant was spiked with ^{137}Cs tracer. Nominal 15 mL simulant was added to ~0.080 g CST (masses determined to nearest 0.0001 g). See Appendix C for specific CST masses and simulant volumes. The contact phase ratios averaged 189 mL solution per g CST. Mixing continued for 95.3 h at 21 °C on the Cole-Parmer orbital shaker. After contact completion, a nominal 2-mL sample aliquot was collected from each process solution and filtered through a 0.45-micron pore size nylon syringe filter. The filtrates were collected for ^{137}Cs analysis.

4.7 Analysis

The samples traced with ^{137}Cs were analyzed using a suite of high-purity lithium drifted germanium gamma detectors. Comparator samples were prepared from aliquots collected from the starting feed matrix and measured identically to the samples. Sample count time was adjusted to achieve an overall statistical count uncertainty of <1%.

The batch distribution coefficients were calculated according to Eq. (4.1).

$$\frac{(A_0 - A_1)}{A_1} \times \frac{V}{M \times F} = K_d \quad (4.1)$$

where A_0 = initial ^{137}Cs concentration (µCi/mL)
A_1 = final (equilibrium) ^{137}Cs concentration (µCi/mL)
V = volume of the batch contact liquid (mL)
M = measured mass CST (g)
F = F-factor, mass of the 105 °C dried CST divided by the mass of the undried CST
K_d = batch-distribution coefficient (mL/g)

Final (equilibrium) Cs concentrations (C_{Eq}) were calculated relative to the tracer recovered in the contacted samples (A_1) and the initial metal concentration (C_0) according to Eq. (4.2).

$$C_0 \times \left(\frac{A_1}{A_0}\right) = C_{Eq} \tag{4.2}$$

where C_0 = initial Cs concentration in solution (µg/mL or M)
C_{Eq} = equilibrium Cs concentration in solution (µg/mL or M)

The equilibrium Cs concentrations loaded onto the CST (Q in units of mmoles Cs per gram of dry CST mass) were calculated according to Eq. (4.3).

$$\frac{C_0 \times V \times \left(1 - \frac{A_1}{A_0}\right)}{M \times F \times 1000 \times FW} = Q \tag{4.3}$$

where Q = equilibrium Cs concentration in the CST (mmole/g CST)
1000 = conversion factor to convert µg to mg
FW = Cs formula weight

5.0 Results

This section provides the testing results for the F-factor evaluation measured at two different temperatures; Cs time to equilibrium test results; Stage 1, 2A, 2B, 3, and AP-107 isotherms; and the precision study with the Baseline simulant. The equilibrium, isotherm, and precision test results are based on the dry CST mass, where the CST was dried to constant mass at 105 °C.

5.1 F-Factor Evaluation

The F-factor was evaluated at 105 °C and 427 °C to assess the best approach to evaluating the F-factor. Because the CST was not pretreated by rinsing with 0.1 M NaOH solution, residual water content from CST contact with rinse solutions was not a confounding issue. Previous studies incorporated rinsing of CST to remove colloidal fines. Therefore, this evaluation was expected to be applicable for the best possible scenario to assess precision.

The F-factor samples were collected just before and after CST subsampling activities for batch contact tests. Thus, each measurement incorporated a duplicate pair. Table 5.1 summarizes the average and relative percent difference (RPD) of the seven duplicate pairs collected for F-factor determination. Figure 5.1 shows the plotted sample data.

Table 5.1. F-Factor Duplicate Average and Relative Percent Difference

CST Lot	2002009604	2002009604	2099000001	2099000001
Temperature	105 °C	427 °C	105 °C	427 °C
Equilibrium testing	0.8699	0.8450	0.8778	0.8499
RPD	*1.61%*	*0.15%*	*1.70%*	*0.11%*
Isotherm Stage 1 simulant testing	0.9202	0.8456	0.9219	0.8512
RPD	*0.14%*	*0.06%*	*0.20%*	*0.14%*
Isotherm all other simulants testing	0.8956	0.8464	--	--
RPD	*0.49%*	*0.08%*	--	--
Precision testing	0.9091	0.8427	0.9128	0.8506
RPD	*1.81%*	*0.23%*	*0.13%*	*0.01%*
Grand average	0.8987	0.8449	0.9042	0.8506
RSD	*2.3%*	*0.19%*	*2.4%*	*0.09%*
n	*8*	*8*	*6*	*6*

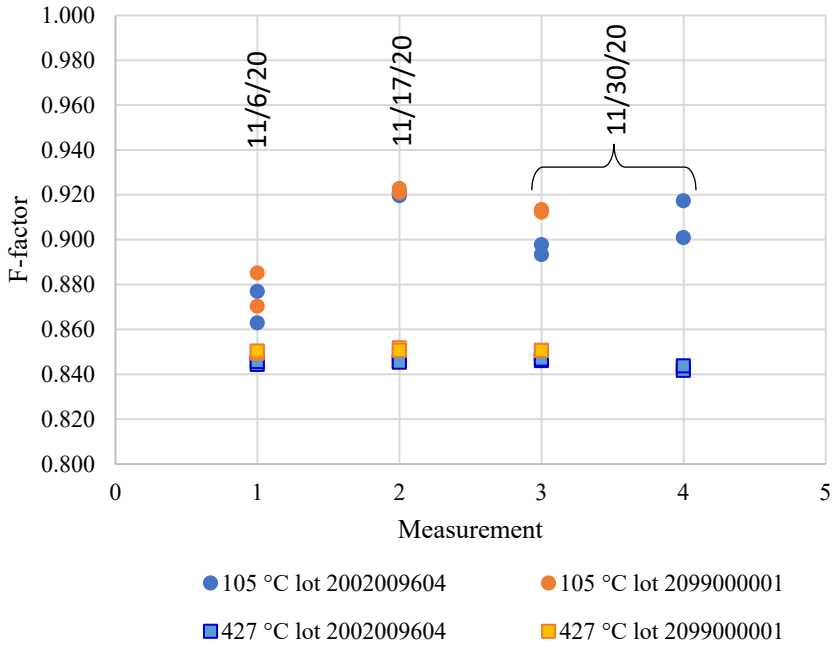

Figure 5.1. Graphical Representation of the F-Factor Precision Study

The CST binder is composed of $Zr(OH)_4$. Exposure to high temperature reorganizes $Zr(OH)_4$ forming ZrO_2 with release of two H_2O (see Fiskum et al. 2019a, Appendix D). The nominal 6.3 wt% mass loss between 105 °C and 427 °C is consistent with the chemical change in the binder (~4.3 wt%). Provided that the F-factor mass basis used for determining the CST bed density and the batch distribution coefficient is constant, the prediction of the 50% Cs breakthrough will not be affected by the selected F-factor temperature. The K_d and Q values will be higher when normalized to F-factors generated at 427 °C relative to F-factors generated at 105 °C.

The relative standard deviation (RSD) of the F-factor measured at 105 °C between sampling days (~2.3% RSD) was about 10× larger than the corresponding deviation for the F-factor measured at 427 °C (0.19% RSD). Drying at 105 °C in the oven resulted in an overall variation of 5% between the maximum and minimum F-factors, where longer heating time generally resulted in lower F-factors, indicative of incremental water loss. Measuring the F-factor at 427 °C has several advantages.

1. Results are rapid and can be obtained within 4 h as opposed to a couple of days.

2. The CST samples are easier to handle in a lidded crucible. The CST is easily statically charged and bounces around in the glass vial with potential for particles to pop out of the glass vial. With a lidded crucible, the CST remains securely in place.

3. Duplicate sample precision and precision across sampling days is generally tighter than that found with the drying to 105 °C.

5.2 TGA results

Figure 5.2 and Figure 5.3 show the TGA weight loss and first-derivative weight loss curves for the two CST lots. Figure 5.2 presents the data as a function of time to show the weight loss events that occur during the isothermal holds at 100 °C and 427 °C. About 4% to 5% of the weight is lost for all samples

while heating to 100 °C and another 2% of weight is lost during the 1-h hold at 100 °C. This observation was consistent with oven drying where extended hold times at 105 °C resulted in incrementally increased mass loss. The samples continued to lose weight while heating to 427 °C, reaching a total of ~15% weight loss by 427 °C. The isothermal hold at 427 °C did not show significant weight loss, nor did further heating to 600 °C. All samples had a final weight loss of 15% to 16%, consistent with the weight loss measured at 427 °C held for 4 h in the furnace. Figure 5.3 presents the weight loss data as a function of temperature in addition to showing the derivative of the weight loss curves. Vertical lines in the weight loss data are due to the isothermal holds at 100 °C and 427 °C. While heating from 100 °C to 427 °C, three distinct peaks can be seen in the derivative weight loss curve, suggesting there are three weight-loss events occurring.

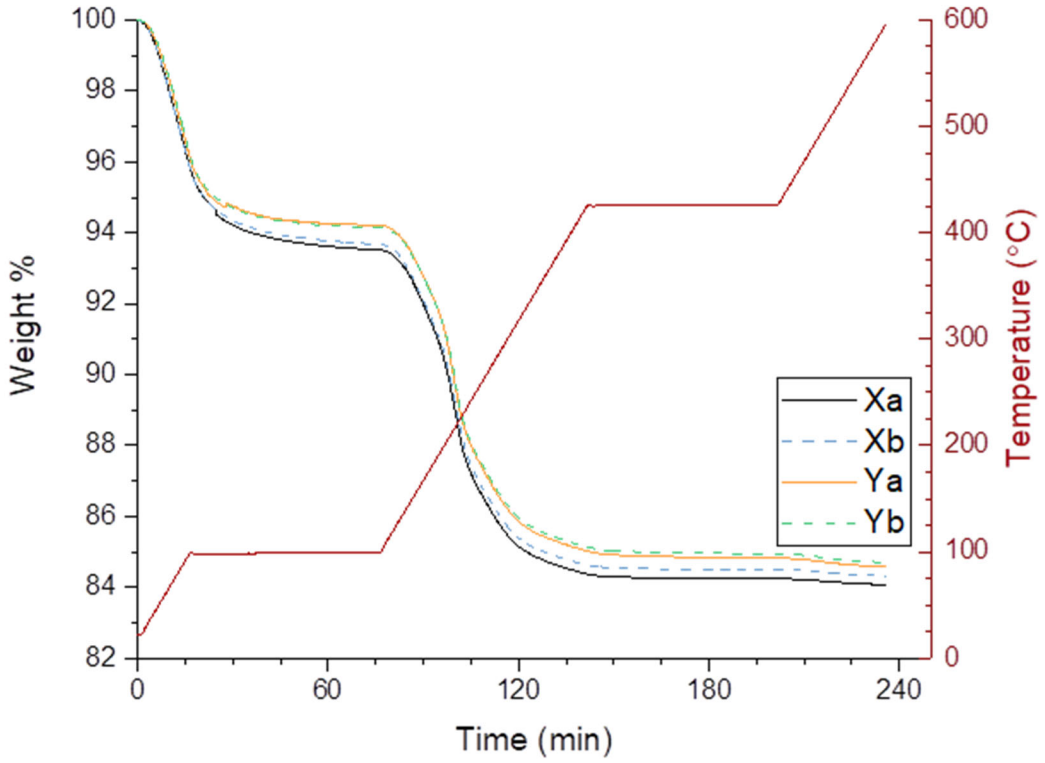

Figure Note: The right-axis shows the temperature program steps overlaid with the data. Samples designated X in the legend are aliquots of lot 2002009604 and Y are aliquots of lot 2099000001. There were no substantial differences in the replicate measurements for each lot.

Figure 5.2. Time-Based Weight Loss of Samples during TGA Measurements

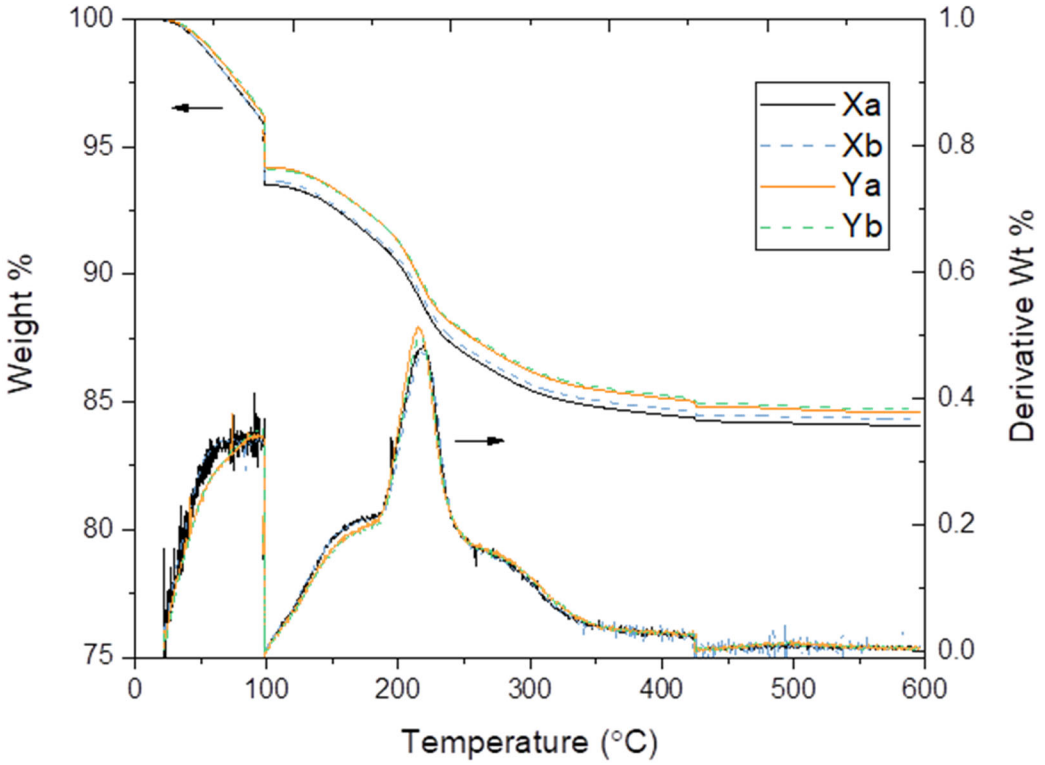

Figure Notes: Samples designated X in the legend are aliquots of lot 2002009604 and Y are aliquots of lot 2099000001. There were no substantial differences in the replicate measurements for each lot.

The arrows point to the relevant axis.

Figure 5.3. Temperature-Based Weight Loss of Samples during TGA Measurements and First-Derivative Weight Loss Curves

5.3 Equilibrium Testing

Figure 5.4 and Figure 5.5 provide the K_d and Q results, respectively, as functions of time. Results were used to establish the contact time required to reach Cs distribution equilibrium in the Stage 1 simulant at both 13 and 21 °C. Underpinning data (C_0, C_1, V, K_d, and Q values) are provided in Appendix A. Figure 5.4 shows that equilibrium K_d was essentially reached at 96 h at contact temperature of 21 °C for lot 2002009604. CST lot 2099000001 K_d values continued to increase through 240 h at 21 °C. Longer contact time (at least ~240 h for lot 2002009604 and ~338 h for lot 2099000001) was needed to reach equilibrium at the 13 °C contact temperature.

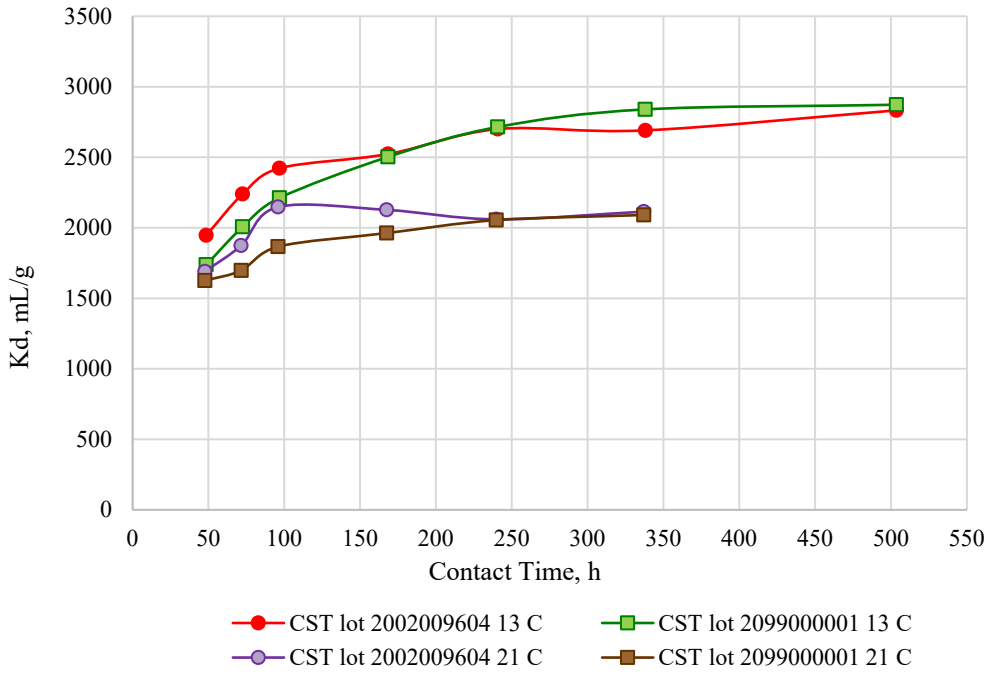

Figure 5.4. Analyte Distribution Coefficient (K_d) as a Function of Time in Stage 1 Simulant, 13 and 21 °C

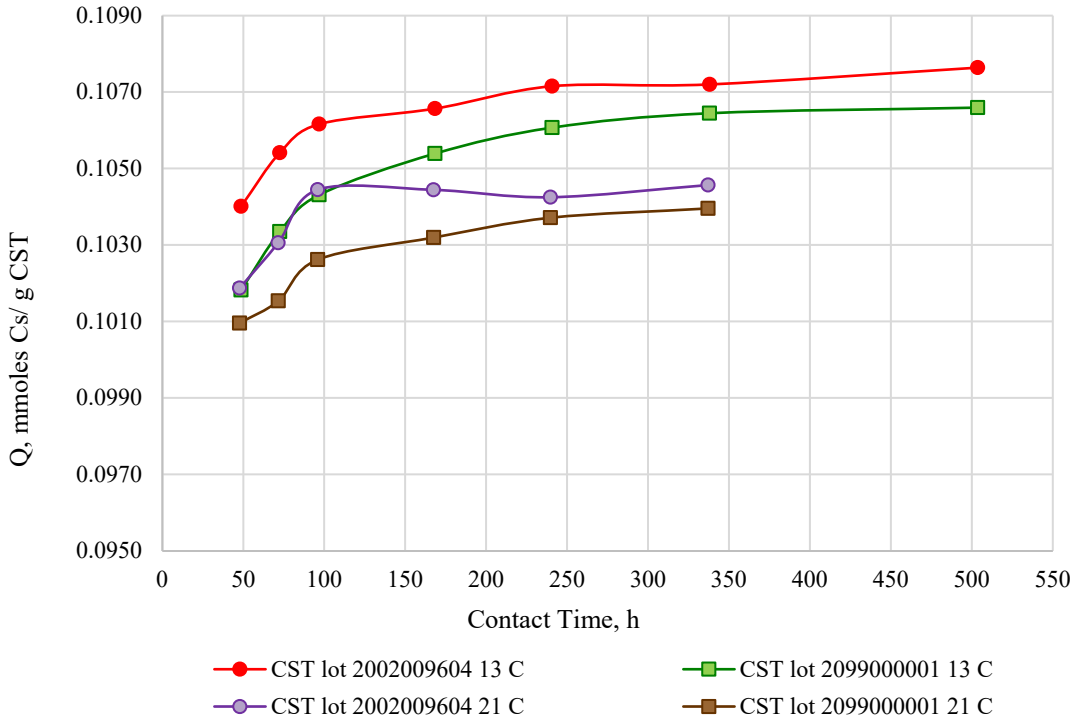

Figure 5.5. Analyte Loading (Q) onto CST as a Function of Time in Stage 1 Simulant, 13 and 21 °C

Figure 5.5 demonstrates CST lot 2002009604 achieved higher Cs capacity and shorter time to reach capacity relative to lot 2099000001 under the processing conditions. However, the final contact time Q values (0.1076 and 0.1066 mmoles Cs/g CST after 504 h 13 °C; 0.1046 and 0.1040 mmoles Cs/g CST after 337 h 21 °C) differed by only 1.0 % or less. This difference is expected to be within the overall experimental uncertainty.

Figure 5.6 and Figure 5.7 show similar K_d and Q values versus time for the Baseline simulant tested at 21 °C for both CST lots. Juxtaposed with the K_d data in Figure 5.6 are previously generated equilibrium data (Fiskum et al. 2019b). The current test indicated that equilibrium was reached at 96-h contact time whereas Fiskum et al. (2019b) showed 48-h contact time would suffice.

A 96-h contact time is conservatively recommended for batch contact testing at 21 °C. A 240-h contact time is recommended for testing at 13 °C. Testing at >21 °C likely could be completed in <96 h.

Clearly the CST capacity for Cs is enhanced in the Stage 1 simulant compared to the Baseline simulant. The Stage 1 simulant K_d values were ~74% higher and the Q values were ~23% higher than those of the Baseline simulant (21 °C). The Stage 1 simulant matrix chemistry appeared to enhance Cs exchange onto CST, as intended.

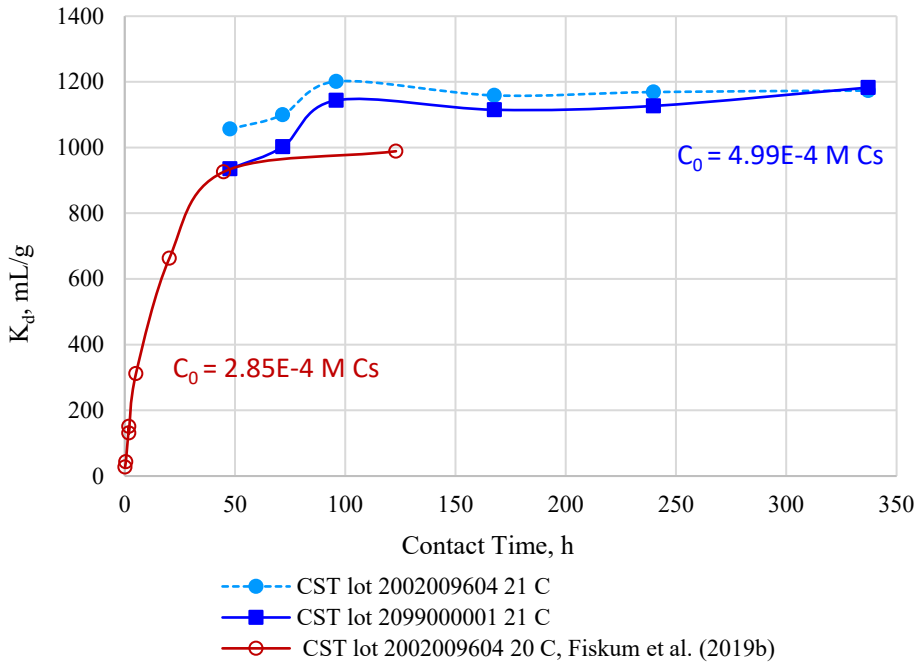

Figure 5.6. Analyte Distribution Coefficient onto CST as a Function of Time in Baseline Simulant

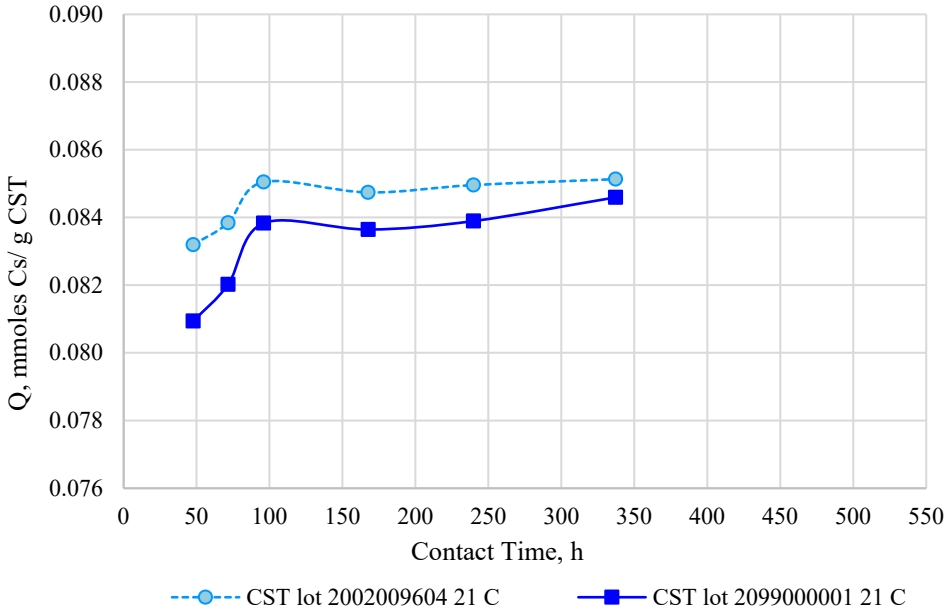

Figure 5.7. Analyte Loading (Q) onto CST as a Function of Time in Baseline Simulant

As previously described by King et al. (2018), when equilibrium Cs distribution is neared and the CST is essentially loaded with Cs, small additional changes in the aqueous Cs concentration can cause significant K_d shifts whereas changes in Q would be minimal. These data demonstrated the maximum change in Q values between 48 h and final contact times was 5%; the maximum change in K_d values between 48 h and final contact times was 65%.

5.4 Isotherm Results from Simulant Stages

Isotherms were generated with all simulants at 13 °C and at least a 238-h contact time. Whereas both CST lots were tested with Stage 1 simulant, only the higher-performing CST lot (2002009604) was tested with the other simulants. The following sections discuss the isotherm test results.

Initial testing with the Stage 1 simulant was conducted to determine which of the two CST lots has the higher Cs capacity at the nominal Cs feed condition of 6.8×10^{-5} M (9.04 µg/mL). Figure 5.8 shows the K_d values versus Cs concentrations, and Figure 5.9 shows the Q values versus Cs concentrations along with the Freundlich/Langmuir Hybrid Equilibrium fits (Hamm et al. 2002). Plotted data are provided in Appendix B.

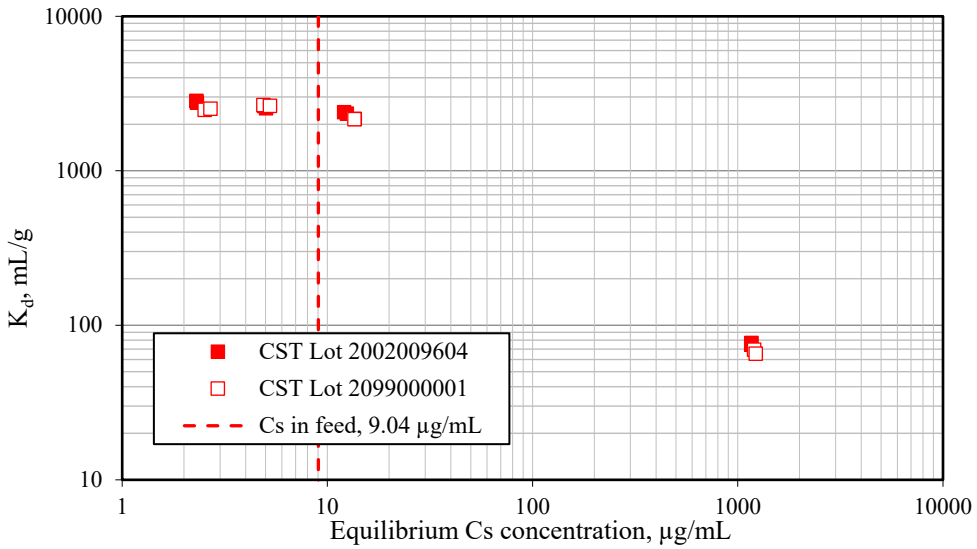

Figure 5.8. Cs K_d vs. Cs Concentration, Stage 1 Simulant

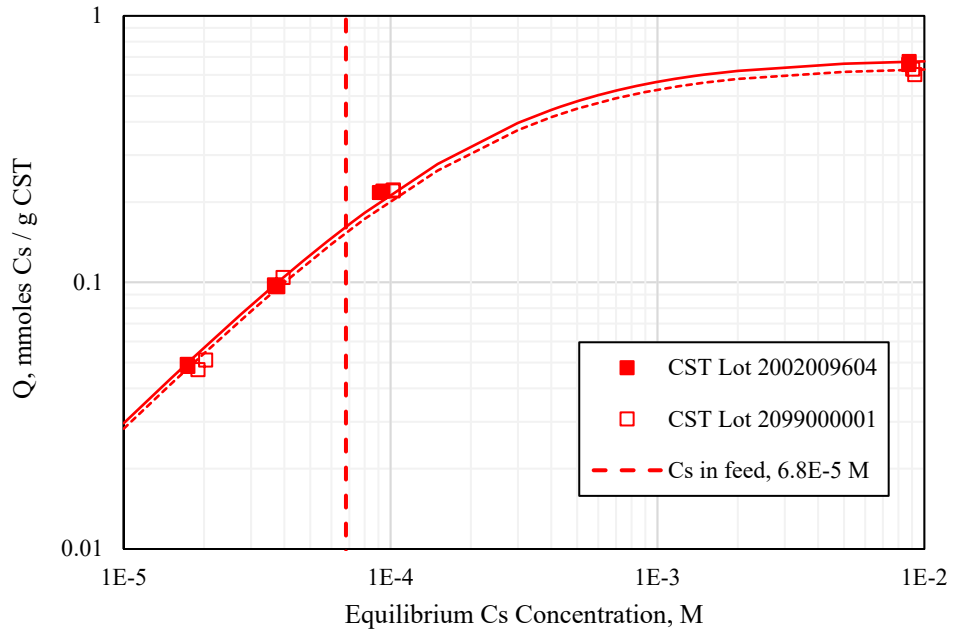

Figure Note: CST lot 2002009604 is represented by the solid curve fit. CST lot 2099000001 is represented by the dashed curve fit.

Figure 5.9. Q vs. Cs Concentration, Stage 1 Simulant with Freundlich/Langmuir Hybrid Equilibrium Fits

The two different lots were largely not distinguishable with respect to K_d and Q values. However, the Cs capacity for CST lot 2002009604 was slightly (5%) higher than that of CST lot 2099000001 (0.161 vs. 0.153 mmoles Cs/g at 6.8×10^{-5} M [9.04 µg/mL] Cs). Thus, CST lot 2002009604 was used for all further isotherm testing in the other simulants. Additionally, because the higher-capacity lot exceeded the threshold of 0.10 mmole Cs/g at 6.8×10^{-5} M Cs, the additional testing of simulants was required as previously described (see Section 3.1). Note that the 0.10 mmole Cs/g limit is defined as 141,600 Ci of cesium loading with a 20% mass fraction ^{137}Cs.

Figure 5.10 provides the K_d values versus equilibrium Cs concentration and Figure 5.11 provides the Q values versus equilibrium Cs concentration for Stage 2A, 2B, 3, and AP-107 simulants. The data underpinning these graphs are provided in Appendix B.

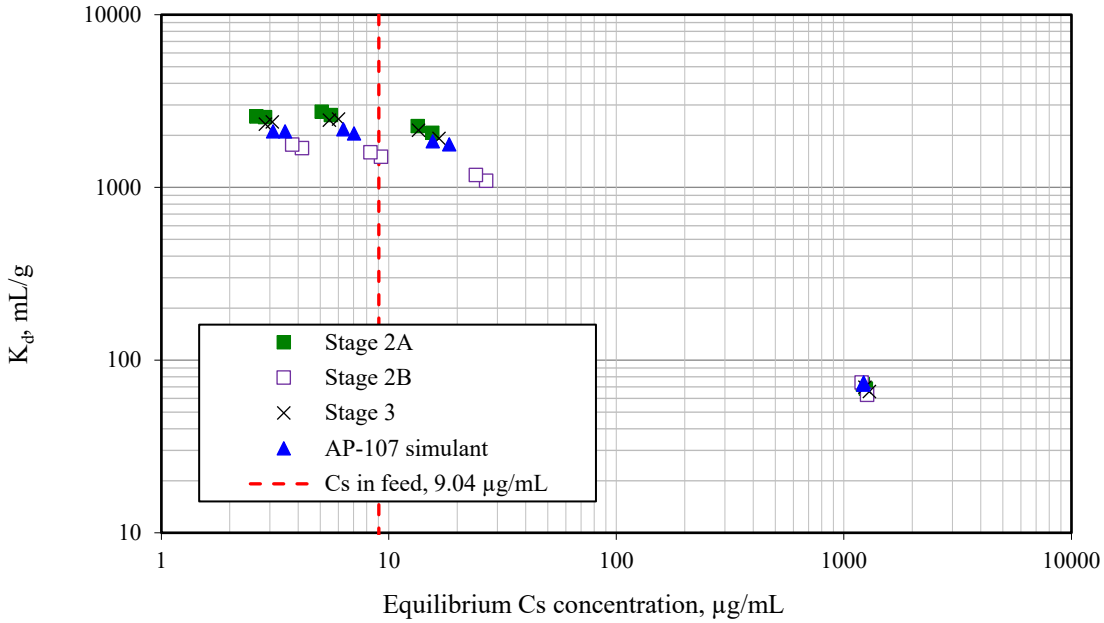

Figure 5.10. Cs K_d vs. Cs Concentration, Stage 2A, 2B, 3, and AP-107 Simulants

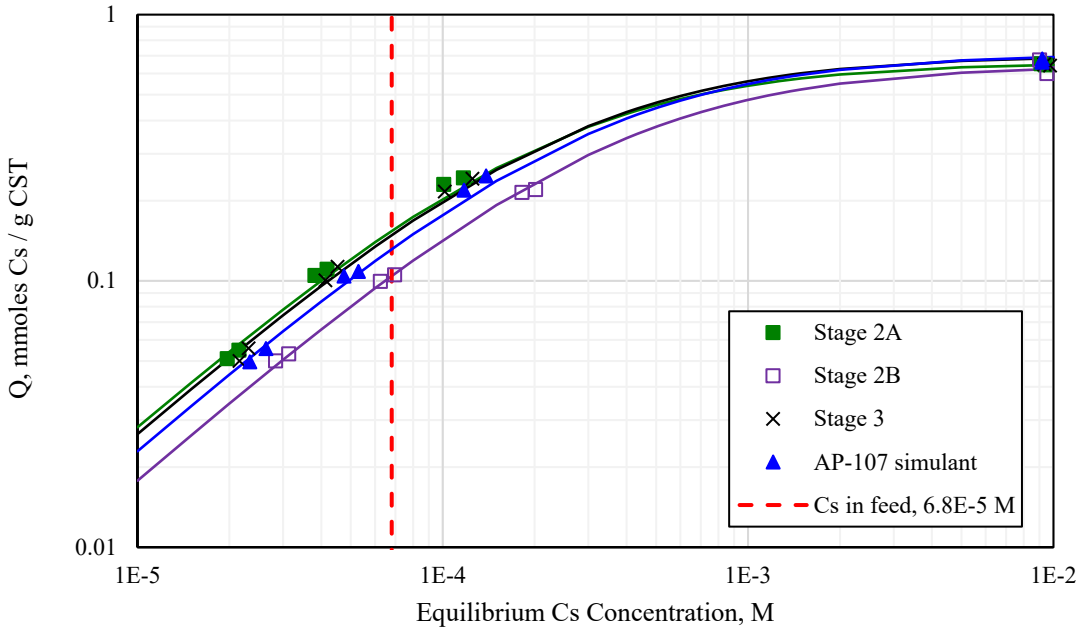

Figure 5.11. Q vs. Cs Concentration, Stage 2A, 2B, 3, and AP-107 Simulants

The AP-107 simulant batch contact results (test conducted at 13 °C) were compared to the actual AP-107 tank waste batch contact test results conducted in-cell at 28 °C (Fiskum et al. 2019a). Table 5.2 compares the compositions of the two matrices; the simulant is clearly bounding with respect to anions and cations that are expected to enhance Cs retention by CST. Figure 5.12 and Figure 5.13 compare the K_d and Q responses as functions of Cs concentration between these two matrices. Clearly the actual tank waste test results met the DSA threshold K_d and Q limits. However, these data are not sufficient to deconvolute the temperature effect from the chemical effect. Additional testing is needed with the actual tank waste at lower temperature to determine if the DSA limits will be met. Based on previous measures of the activation energy for the equilibrium constants for cesium loading, it is anticipated that the actual waste loading at 13 °C will be closer to the actual waste loading at 28 °C than it will be to the simulant loading at 13 °C.

Table 5.2. AP-107 Simulant and Actual Tank Waste Composition Comparison

Matrix Component	AP-107 Simulant, M	AP-107 Tank Waste, M	Comment
Na^+	5.06	5.97[(a)]; 5.48[(b)]	Lower [Na] increases Cs capacity
K^+	0.0757	0.120[(a)]; 0.100[(b)]	Lower [K] increases Cs capacity
NO_3^-	1.60	1.71[(b)]	Lower [NO_3^-] increases Cs capacity
F^-	0.0308	0.0274[(c)]	Higher [F] increases Cs capacity
SO_4^{2-}	0.0627	0.0159[(b)]	Higher [SO_4^{2-}] increases Cs capacity
OH^-	1.01	0.89[(a)]; 0.99[(b)]	Higher [OH^-] increases Cs capacity
NO_2^-	0.944	1.14[(b)]	Lower [NO_2^-] increases Cs capacity
CO_3^{2-}	0.714	0.65[(a)]; 0.635[(b)]	Higher [CO_3^{2-}] increases Cs capacity

(a) Fiskum et al. (2019a)
(b) Rovira et al. (2018)
(c) Rasmussen (2019)

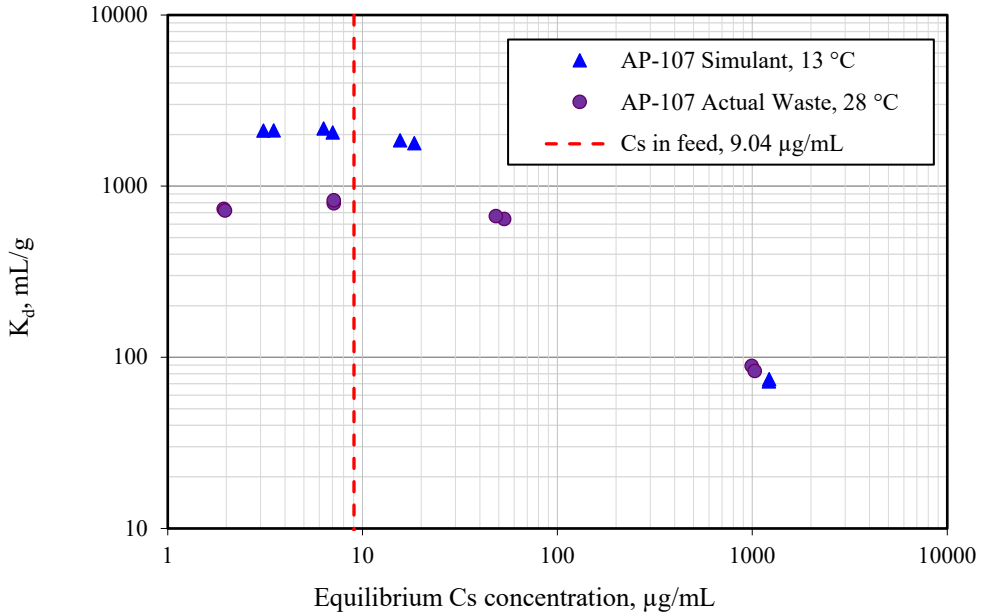

Figure 5.12. K_d vs. Cs Concentration, AP-107 Simulant and AP-107 Tank Waste

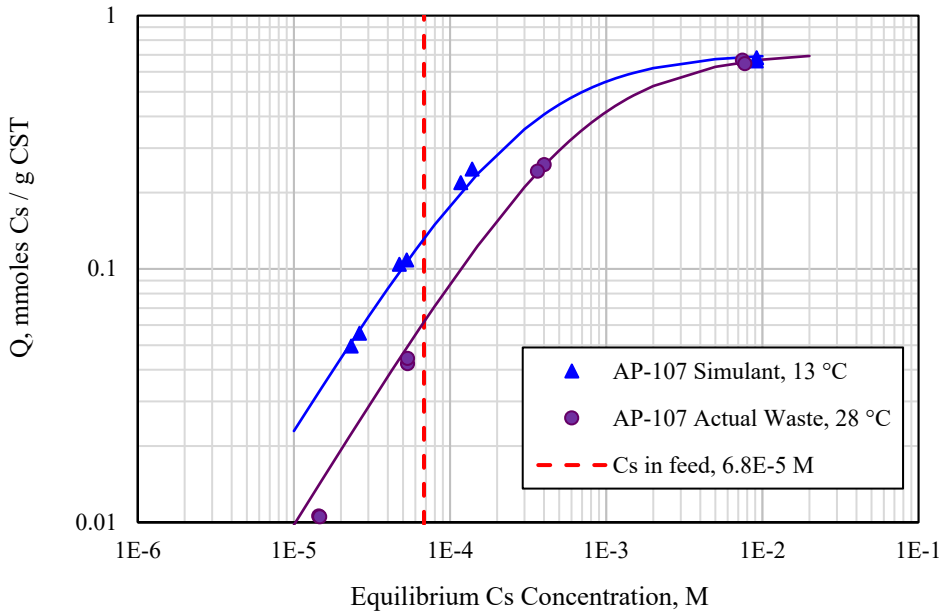

Figure 5.13. Q vs. Cs Concentration, AP-107 Simulant and AP-107 Tank Waste

Table 5.3 provides a summary of the K_d and Q values at the feed condition, 6.8×10^{-5} M Cs. Also provided are the isotherm parameters α_i and β, which are calculated based on the Freundlich/Langmuir Hybrid equilibrium isotherm model (see Hamm et al. 2002) according to Eq. (5.1). The α_i parameter represents the maximum Cs capacity in the CST and the β parameter incorporates the selectivity coefficients, making it dependent on temperature and liquid composition of all the ionic species in solution; the larger the beta parameter, the less favorable (and lower loadings) an isotherm will be.

$$\frac{\alpha_i \times [Cs]}{(\beta + [Cs])} = Q \qquad (5.1)$$

Table 5.3. Summary K_d and Q Values at 6.8×10^{-5} M Cs for CST Lot 2002009604

Matrix	K_d, mL/g[(b)]	Q, mmoles/g	α_i, mmoles Cs/g CST	β, Cs M
DSA threshold	1470	0.100	na	na
Stage 1 simulant	2374	0.161	0.690	2.23E-04
Stage 2A simulant	2262	0.154	0.662	2.25E-04
Stage 2B simulant	1533	0.104	0.647	3.54E-04
Stage 3 simulant	2183	0.148	0.704	2.54E-04
AP-107 simulant	1933	0.131	0.713	3.01E-04
AP-107 tank waste[(a)]	906	0.062	0.718	7.25E-04

(a) Test conducted at 28 °C; calculated values for 6.85×10^{-5} M Cs (Fiskum et al. 2019a).
(b) K_d calculated (Q [mmoles/g] divided by 6.8×10^{-5} mmoles/mL).

All simulants exceeded the threshold 1470 mL/g K_d value and 0.10 mmole Cs/g CST Q values at the nominal feed condition of 6.8×10^{-5} M Cs. Thus, all five additional simulant compositions failed to demonstrate compliance with the upper bound defined by the DSA. The Stage 2B simulant with high K^+ came the closest to meeting the DSA limit. Table 5.4 shows the maximum feed Cs concentrations that

would accommodate the DSA limit for each of the tested simulants. Although each simulant exceeded the upper bound at the nominal Cs concentration (6.8×10^{-5} M) some feeds may meet the DSA limit if the actual Cs concentration does not exceed the concentrations shown in Table 5.4.

Table 5.4. Maximum Feed Cs Concentration to Reach DSA Limit in Bounding Simulants

Matrix	Maximum Cs, M[(a)]
Stage 1 simulant	3.88E-05
Stage 2A simulant	4.00E-05
Stage 2B simulant	6.80E-05
Stage 3 simulant	4.33E-05
AP-107 simulant	4.90E-05
(a) Where Q = 0.10 mmoles/g	

Actual tank waste tests are recommended to establish CST Cs loading in compliance with the DSA. Further studies of temperature effects and specific anionic and cationic matrix effects on Cs exchange onto CST are also recommended to determine the more limiting matrix conditions.

6.0 Precision Testing with Baseline Simulant

The precision of K_d and Q measurements was evaluated for both CST lots 2002009604 and 2099000001, each in triplicate, using the Baseline simulant (5.0×10^{-4} M Cs). Table 6.1 summarizes the measured K_d and Q values along with the average and RSD; underpinning data are provided in Appendix C. The ^{137}Cs tracer in the feed and post-contacted samples was measured by gamma energy analysis. This technique allowed counting to continue until a low statistical uncertainty (<1%) was achieved; this measurement was not confounded by the high salt matrix conditions. These advantages are not available to analysis by ICP-OES or ICP-MS. The RSDs of the triplicate K_d values were well within the overall experimental uncertainties.

Table 6.1. Precision Assessment for K_d and Q Determinations

K_d, mL/g	Average	RSD	Q, mmoles /g	Average	RSD
			CST Lot 2002009604		
1158			8.44E-02		
1153	1161	0.8%	7.83E-02	8.18E-02	3.8%
1172			8.28E-02		
			CST Lot 2099000001		
1053			7.88E-02		
1038	1040	1.2%	7.86E-02	7.94E-02	1.6%
1028			8.08E-02		

7.0 Conclusions

Five simulants were formulated with the chemical compositions bounding the DFLAW tank waste feed campaigns with the intention of achieving maximum Cs loading onto the CST. One simulant, Stage 1, was tested to establish contact time required to reach equilibrium at 13 °C and 21 °C. Five simulants were tested to determine Cs loading onto CST at the equilibrium Cs concentration of 6.8×10^{-5} M at which the DSA limitation was applicable. The testing was meant to demonstrate that Cs loading would remain less than 0.10 mmole Cs per gram CST, corresponding to a maximum TSCR column loading of 141,600 Ci (^{137}Cs). Initial testing was conducted on two CST lots, the higher-capacity lot was forwarded for additional testing. The following conclusions were drawn.

1. There was a lot-to-lot variation on time to reach equilibrium. CST lot 2002009604 appeared to attain equilibrium sooner than lot 2099000001 at 13 °C (240 h vs. 350 h) and 21 °C (96 h vs 240 h).

2. Time to reach equilibrium Cs distribution was temperature-dependent; 96 h contact time was needed at 21 °C and 240 h contact was time needed at 13 °C, each tested with Stage 1 bounding simulant with lot 2002009604.

3. CST lot 2002009604 had slightly (5%) higher Cs capacity than CST lot 2099000001 at the equilibrium feed condition of 6.8×10^{-5} M Cs.

4. All five simulants contacted with CST lot 2002009604 at 13 °C exceeded the DSA limit of 0.10 mmoles Cs loading per g CST.

Additional testing was conducted with the Baseline simulant (Russell et al. 2017) that has been used to confirm CST Cs removal efficacy on CST production lots by Honeywell UOP. Time required to reach equilibrium at 21 °C was established and K_d precision based on triplicate analyses was determined for two different CST lots. The following conclusions were drawn.

1. Equilibrium Cs distribution was complete at 96 h and did not appear to be lot-dependent in this matrix.

2. The K_d precision resulted in 0.8% and 1.2% RSD for the two sets of triplicate results where measurements were based on ^{137}Cs tracer analysis by gamma energy analysis. This precision is very tight and may not be attainable by analysis conducted by other methods (e.g., ICP-MS).

An additional area of interest was associated with the assessment of the F-factor (mass of dry CST divided by the mass of sampled, undried CST). Many measurements to date have been taken based on drying to 105 °C and other measurements based on CST drying to 427 °C. Seven duplicate sample pairs collected over a 3-week period were evaluated at each drying condition. The following conclusions were made.

1. Drying at 427 °C resulted in a tighter duplicate precision than drying at 105 °C (≤0.61% vs. ≤1.8%, respectively) and overall tighter population precision (≤0.28% vs ≤2.3%, respectively).

2. Drying at 427 °C can be accomplished in 4 h, possibly less. Drying at 105 °C likely takes significantly longer (e.g., a day or two).

3. It was not clear what the source of water evolution was at the higher temperature, but destruction of the $Zr(OH)_4$ binder cannot be discounted.

Recommendations

Because the simulant compositions bounding the DFLAW resulted in higher loadings than can be accepted in the DSA for the initial feeds to TSCR, two options should be considered, as follows.

1. Conduct testing on actual tank waste at the bounding contact temperature of 13 °C. Given batch contact logistics (long contact times at chilled condition), this activity will likely be best approached by testing Cs-decontaminated tank waste outside of the hot cells. This approach preserves the matrix while minimizing the material dose rate.

2. Determine specific impacts of anions and cations on Cs uptake onto CST. The effect of individual key anions (carbonate, sulphate, fluoride, nitrate, nitrite, and hydroxide) and a more focused study on sodium and potassium (within the tank waste concentration ranges) on Cs uptake can be conducted by parametric testing in a very simple simulant. This effort would create a better understanding of the magnitude of the matrix drivers for Cs uptake. Understanding the enhancement effect matrix components have on Cs exchange may reduce the need for testing all individual tank wastes and help guide strategies regarding future tank waste blending.

8.0 References

Anderson K. 2020. *Tank Side Cesium Removal Safety Basis Requirement Decision Document*. RPP-RPT-62225, Rev. 0. Washington River Protection Solutions, Richland, Washington.

ASME. 2000. *Quality Assurance Requirements for Nuclear Facility Applications*. NQA-1-2000. The American Society of Mechanical Engineers, New York, New York.

ASME. 2008. *Quality Assurance Requirements for Nuclear Facility Applications*. NQA-1-2008. The American Society of Mechanical Engineers, New York, New York.

ASME. 2009. *Addenda to ASME NQA-1-2008*. NQA-1a-2009. The American Society of Mechanical Engineers, New York, New York.

Bernards JK, TM Hohl, RT Jasper, N Pak, SD Reaksecker, AJ Schubick, LM Bergmann, AN Praga, and SN Tilanus. 2018. *TOPSim Model Requirements Document*. RPP-RPT-59470, Rev. 2. Washington River Protection Solutions, Richland, Washington.

Braun R, TJ Dangieri, DJ Fennelly, JD Sherman, WC Schwerin, RR Willis, NE Brown, JE Miller, RG Anthony, CV Philip, LA Bray, GN Brown, DD Lee, TT Borek, and WJ Connors. 1996. "Ion Exchange Performance of Commercial Crystalline Silicotitanates for Cesium Removal." *Spectrum '96, Proceedings – International Topical Meeting on Nuclear and Hazardous Waste Management*. SAND-96-0656C; CONF-960212-65. Sandia National Laboratories, Albuquerque, New Mexico.

Bromley LA. 1973. "Thermodynamic Properties of Strong Electrolytes in Aqueous Solutions", AIChE Journal, 19(2), 313-320.

Brown GN, LA Bray, CD Carlson, KJ Carson, JR DesChane, RJ Elovich, FV Hoopes, DE Kurath, LL Nenninger, and PK Tanaka. 1996. *Comparison of Organic and Inorganic Ion Exchangers for Removal of Cesium and Strontium from Simulated and Actual Hanford 241-AW-101 DSSF Tank Waste*. PNNL-11120. Pacific Northwest National Laboratory, Richland, Washington.

Fiskum SK, AM Rovira, HA Colburn, AM Carney, and RA Peterson. 2019a. *Cesium Ion Exchange Testing Using a Three-Column System with Crystalline Silicotitanate and Hanford Tank Waste 241-AP-107*. PNNL-28958, Rev. 0; RPT-DFTP-013, Rev. 0. Pacific Northwest National Laboratory, Richland, Washington.

Fiskum SK, AM Rovira, JR Allred, HA Colburn, MR Smoot, AM Carney, TT Trang-Le, MG Cantaloub, EC Buck, and RA Peterson. 2019b. *Cesium Removal from Tank Waste Simulants Using Crystalline Silicotitanate at 12% and 100% TSCR Bed Heights*. PNNL-28527, Rev. 0; RPT-TCT-001, Rev. 0. Pacific Northwest National Laboratory, Richland, Washington.

Fondeur, FF, T Hang, MP Bussey, WR Wilmarth, DD Walker, and SD Fink. 2000. *The Effect of Carbonate, Oxalate and Peroxide on the Cesium Loading of Ionsiv® IE-910 and IE-911*. WSRC-TR-2000-00344. Westinghouse Savannah River Company Aiken, South Carolina

Hamm LL, T Hang, DJ McCabe, and WD King. 2002. *Preliminary Ion Exchange Modeling for Removal of Cesium from Hanford Waste Using Hydrous Crystalline Silicotitanate Material*. WSRC-TR-2001-00400. Westinghouse Savannah River Company, Aiken, South Carolina.

King WD, LL Hamm, DJ McCabe, CA Nash, and FF Fondeur. 2018. *Crystalline Silicotitanate Ion Exchange Media Long-Term Storage Evaluation*. SRNL-STI-2018-00567, Rev. 0. Savannah River National Laboratory, Aiken, South Carolina.

Pease LF, SK Fiskum, HA Colburn, and PP Schonewill. 2019. *Cesium Ion Exchange with Crystalline Silicotitanate: Literature Review*. PNNL-28343, Rev. 0; RPT-LPTTS-001, Rev. 0. Pacific Northwest National Laboratory, Richland, Washington.

Rasmussen JH. 2019. *Derivation of Best-Basis Inventory for Tank 241-AP-107 as of January 1, 2019*. RPP-RPT-48103, Rev. 11. Washington River Protection Solutions, Richland, Washington.

Rovira AM, SK Fiskum, HA Colburn, JR Allred, MR Smoot, and RA Peterson. 2018. *Cesium Ion Exchange Testing Using Crystalline Silicotitanate with Hanford Tank Waste 241-AP-107*. PNNL-27706; RPT-DFTP-011, Rev. 0, Pacific Northwest National Laboratory, Richland, Washington.

Russell RL, PP Schonewill, and CA Burns. 2017. *Simulant Development for LAWPS Testing*. PNNL-26165, Rev. 0; RPT-LPIST-001, Rev. 0. Pacific Northwest National Laboratory, Richland, Washington.

Siewart J. 2019. *Tank Side Cesium Removal (TSCR) IXC-150 Sizing*. RPP-CALC-62497, Rev 2. Washington River Protection Solutions, Richland, Washington.

Zheng Z, RG Anthony, and JE Miller. 1997. “Modeling Multicomponent Ion Exchange Equilibrium Utilizing Hydrous Crystalline Silicotitanates by a Multiple Interactive Ion Exchange Site Model.” *Industrial & Engineering Chemistry Research* 36(6):2427-2434.

Appendix A – Equilibrium Testing Batch Contact Results

The following tables provide test detail and results that are plotted in Figure 5.4 through Figure 5.7. The dry crystalline silicotitanate (CST) mass is based on the 105 °C drying temperature. For lot 2002009604, the F-factor was 0.8699 and for lot 2099000001 the F-factor was 0.8778. Using the higher 427 °C drying temperature decreases the F-factor. For lot 2002009604, the 427 °C F-factor was 0.8450 (3.0% reduction) and for lot 2099000001 the F-factor was 0.8477 (3.3% reduction). Applying the lower F-factor values will increase K_d and Q values corresponding to the F-factor percent change. The fourth significant digit in the Q values is shown for information only.

Table A.1. Stage 1 Cs Equilibrium Testing Results, CST Lot 2002009604, 13 °C

Stage 1 Simulant, 5.57E-4 M Cs (C_0), 1.0179 g CST (105 °C dry mass basis)				
Time, h	Volume, mL	Eq. Cs M (C_1)	K_d, mL/g	Q, mmoles/g
49	210	5.33E-05	1947	1.040E-01
73	208	4.65E-05	2240	1.054E-01
97	206	4.29E-05	2423	1.062E-01
168	204	4.09E-05	2523	1.066E-01
241	202	3.81E-05	2700	1.072E-01
338	200	3.79E-05	2691	1.072E-01
504	198	3.57E-05	2833	1.076E-01

Table A.2. Stage 1 Cs Equilibrium Testing Results, CST Lot 2099000001, 13 °C

Stage 1 Simulant, 5.57E-4 M Cs (C_0), 1.0473 g CST (105 °C dry mass basis)				
Time, h	Volume, mL	Eq. Cs M (C_1)	K_d, mL/g	Q, mmoles/g
49	210	5.81E-05	1738	1.018E-01
73	208	5.06E-05	2007	1.034E-01
97	206	4.59E-05	2212	1.043E-01
168	204	4.06E-05	2503	1.054E-01
241	202	3.73E-05	2716	1.061E-01
338	200	3.54E-05	2840	1.064E-01
504	198	3.47E-05	2873	1.066E-01

Table A.3. Stage 1 Cs Equilibrium Testing Results, CST Lot 2002009604, 21 °C

Stage 1 Simulant, 5.57E-4 M Cs (C_0), 1.0252 g CST (105 °C dry mass basis)				
Time, h	Volume, mL	Eq. Cs M (C_1)	K_d, mL/g	Q, mmoles/g
48	210	6.02E-05	1691	1.019E-01
72	208	5.44E-05	1875	1.031E-01
96	206	4.76E-05	2148	1.044E-01
168	204	4.76E-05	2128	1.044E-01
240	202	4.86E-05	2061	1.043E-01
337	200	4.70E-05	2115	1.046E-01

Table A.4. Stage 1 Cs Equilibrium Testing Results, CST Lot 2099000001, 21 °C

Stage 1 Simulant, 5.57E-4 M Cs (C_0), 1.0477 g CST (105 °C dry mass basis)				
Time, h	Volume, mL	Eq. Cs M (C_1)	K_d, mL/g	Q, mmoles/g
48	210	6.19E-05	1626	1.010E-01
72	208	5.91E-05	1698	1.015E-01
96	206	5.38E-05	1867	1.026E-01
168	204	5.09E-05	1962	1.032E-01
240	202	4.84E-05	2055	1.037E-01
337	200	4.72E-05	2091	1.040E-01

Table A.5. Baseline Cs Equilibrium Testing Results, CST Lot 2002009604, 21 °C

Baseline Simulant, 4.99E-4 M Cs (C_0), 1.0322 g CST (105 °C dry mass basis)				
Time, h	Volume, mL	Eq. Cs M (C_1)	K_d, mL/g	Q, mmoles/g
48	205	7.88E-05	1057	8.320E-02
72	202	7.56E-05	1100	8.384E-02
96	201	6.95E-05	1201	8.505E-02
168	199	7.10E-05	1159	8.474E-02
240	197	6.99E-05	1169	8.496E-02
337	195	6.91E-05	1174	8.513E-02

Table A.6. Baseline Cs Equilibrium Testing Results, CST Lot 2099000001, 21 °C

Baseline Simulant, 4.99E-4 M Cs (C_0), 1.0564 g CST (105 °C dry mass basis)				
Time, h	Volume, mL	Eq. Cs M (C_1)	K_d, mL/g	Q, mmoles/g
48	204	8.68E-05	935	8.094E-02
72	202	8.13E-05	1003	8.203E-02
96	200	7.21E-05	1144	8.383E-02
168	198	7.30E-05	1115	8.365E-02
240	196	7.17E-05	1127	8.390E-02
337	194	6.82E-05	1183	8.459E-02

Appendix B – Isotherm Batch Contact Results

Table B.1 provides the results used to produce the isotherms in Figure 5.8 and Figure 5.9. The dry CST mass was based on the 105 °C drying temperature (lot 2002009604 F-factor 0.9202; lot 2099000001 F-factor 0.9219). Using the higher 427 °C drying temperature decreased the F-factor ~8.6% (lot 2002009604 0.8456; lot 2099000001 0.8512). Thus, applying the 427 °C F-factor would increases K_d and Q values by ~8.6%.

Table B.1. Stage 1 Simulant Isotherm Data

Sample ID	Dry CST mass, g	Simulant Vol. mL	Initial Cs Conc., M	Equil. Cs Conc., M	K_d, mL/g	Q, mmoles Cs/g
CST Lot 2002009604						
TI104S1-1X	0.0801	15.0	2.76E-04	1.74E-05	2756	4.84E-02
TI104S1-2X	0.0807	15.0	5.56E-04	3.70E-05	2622	9.64E-02
TI104S1-3X	0.0799	15.1	1.24E-03	9.09E-05	2396	2.17E-01
TI104S1-4X	0.0785	15.2	1.23E-02	8.78E-03	77	6.73E-01
TI104S1-1Xd	0.0789	15.0	2.76E-04	1.73E-05	2834	4.92E-02
TI104S1-2Xd	0.0807	15.0	5.56E-04	3.78E-05	2538	9.62E-02
TI104S1-3Xd	0.0792	15.2	1.24E-03	9.36E-05	2346	2.20E-01
TI104S1-4Xd	0.0815	15.2	1.23E-02	8.74E-03	75	6.55E-01
CST Lot 2099000001						
TI104S1-1Y	0.0816	14.9	2.76E-04	1.90E-05	2475	4.70E-02
TI104S1-2Y	0.0793	14.9	5.56E-04	3.67E-05	2659	9.79E-02
TI104S1-3Y	0.0778	15.2	1.24E-03	1.02E-04	2160	2.22E-01
TI104S1-4Y	0.0773	15.2	1.23E-02	9.05E-03	69	6.30E-01
TI104S1-1Yd	0.0753	15.1	2.76E-04	2.03E-05	2516	5.11E-02
TI104S1-2Yd	0.0752	15.2	5.56E-04	3.96E-05	2630	1.04E-01
TI104S1-3Yd	0.0774	15.0	1.24E-03	1.02E-04	2155	2.20E-01
TI104S1-4Yd	0.0769	15.1	1.23E-02	9.21E-03	65	6.01E-01

Table B.2 through Table B.5 provide the results used to produce the isotherms in Figure 5.10 and Figure 5.11 with CST lot 2002009604. Table B.5 data are also used in Figure 5.12 and Figure 5.13. The dry CST mass for the simulant studies is based on the 105 °C drying temperature (F-factor 0.8956). Using the higher 427 °C drying temperature decreases the F-factor to 0.8427 and increases K_d and Q values by ~6.2%.

Table B.2. Stage 2A Simulant Isotherm Data

Sample ID	Dry CST mass, g	Simulant Vol. mL	Initial Cs Conc., M	Equil. Cs Conc., M	K_d, mL/g	Q, mmoles Cs/g
TI104S2a-1X	0.0730	15.3	2.84E-04	2.15E-05	2559	5.49E-02
TI104S2a-2X	0.0730	15.1	5.78E-04	4.18E-05	2627	1.11E-01
TI104S2a-3X	0.0727	15.4	1.27E-03	1.17E-04	2074	2.43E-01
TI104S2a-4X	0.0727	15.5	1.24E-02	9.41E-03	68	6.47E-01
TI104S2a-1Xd	0.0721	13.9	2.84E-04	1.97E-05	2578	5.10E-02
TI104S2a-2Xd	0.0729	14.1	5.78E-04	3.82E-05	2749	1.05E-01
TI104S2a-3Xd	0.0732	14.5	1.27E-03	1.01E-04	2268	2.30E-01
TI104S2a-4Xd	0.0736	14.4	1.24E-02	9.12E-03	72	6.53E-01

Table B.3. Stage 2B Simulant Isotherm Data

Sample ID	Dry CST mass, g	Simulant Vol. mL	Initial Cs Conc., M	Equil. Cs Conc., M	K_d, mL/g	Q, mmoles Cs/g
TI104S2b-1X	0.0725	15.2	2.85E-04	3.13E-05	1691	5.32E-02
TI104S2b-2X	0.0721	15.2	5.69E-04	6.96E-05	1507	1.05E-01
TI104S2b-3X	0.0733	15.4	1.25E-03	2.02E-04	1094	2.20E-01
TI104S2b-4X	0.0723	15.5	1.23E-02	9.54E-03	63	6.00E-01
TI104S2b-1Xd	0.0734	14.3	2.85E-04	2.83E-05	1771	5.01E-02
TI104S2b-2Xd	0.0727	14.3	5.69E-04	6.25E-05	1598	9.95E-02
TI104S2b-3Xd	0.0723	14.5	1.25E-03	1.82E-04	1183	2.15E-01
TI104S2b-4Xd	0.0727	14.8	1.23E-02	9.02E-03	74	6.75E-01

Table B.4. Stage 3 Simulant Isotherm Data

Sample ID	Dry CST mass, g	Simulant Vol. mL	Initial Cs Conc., M	Equil. Cs Conc., M	K_d, mL/g	Q, mmoles Cs/g
TI104S3-1X	0.0727	15.2	2.90E-04	2.31E-05	2399	5.59E-02
TI104S3-2X	0.0731	15.3	5.85E-04	4.52E-05	2491	1.13E-01
TI104S3-3X	0.0727	15.3	1.28E-03	1.25E-04	1924	2.42E-01
TI104S3-4X	0.0726	15.5	1.28E-02	9.75E-03	66	6.44E-01
TI104S3-1Xd	0.0731	13.6	2.90E-04	2.16E-05	2326	5.01E-02
TI104S3-2Xd	0.0736	13.6	5.85E-04	4.13E-05	2456	1.01E-01
TI104S3-3Xd	0.0733	13.5	1.28E-03	1.02E-04	2146	2.17E-01
TI104S3-4Xd	0.0727	13.7	1.28E-02	9.32E-03	70	6.51E-01

Table B.5. AP-107 Simulant Isotherm Data

Sample ID	Dry CST mass, g	Simulant Vol. mL	Initial Cs Conc., M	Equil. Cs Conc., M	K_d, mL/g	Q, mmoles Cs/g
TI104S107-1X	0.0718	15.2	2.90E-04	2.63E-05	2114	5.58E-02
TI104S107-2X	0.0721	15.2	5.67E-04	5.29E-05	2058	1.09E-01
TI104S107-3X	0.0727	15.4	1.31E-03	1.39E-04	1782	2.48E-01
TI104S107-4X	0.0724	15.4	1.24E-02	9.19E-03	74	6.82E-01
TI104S107-1Xd	0.0725	13.5	2.90E-04	2.33E-05	2114	4.97E-02
TI104S107-2Xd	0.0722	14.5	5.67E-04	4.75E-05	2174	1.04E-01
TI104S107-3Xd	0.0727	13.4	1.31E-03	1.17E-04	1852	2.19E-01
TI104S107-4Xd	0.0717	14.7	1.24E-02	9.16E-03	72	6.63E-01

Appendix C – Precision Study Batch Contact Results

Table C.1 provides the results used to produce the data summarized in Table 6.1. The dry CST mass is based on the 105 °C drying temperature. Using the higher 427 °C drying temperature decreases the F-factor and increases K_d and Q values by ~7.3% for each CST lot. The relevant F-factors for each CST lot are provided in Table C.1.

Table C.1. Baseline Simulant Precision Analysis Data

Sample ID	Dry CST mass, g	Simulant Vol. mL	Initial Cs Conc., M	Equil. Cs Conc., M	K_d, mL/g	Q, mmoles Cs/g
CST Lot 2002009604[(a)]						
TI105B-X1	0.0762	15.1	4.99E-04	7.28E-05	1158	8.44E-02
TI105B-X2	0.0830	15.1	4.99E-04	6.80E-05	1153	7.83E-02
TI105B-X3	0.0776	15.0	4.99E-04	7.06E-05	1172	8.28E-02
CST Lot 2099000001[(b)]						
TI105B-Y1	0.0811	15.0	4.99E-04	7.39E-05	1053	7.88E-02
TI105B-Y2	0.0816	15.2	4.99E-04	7.55E-05	1038	7.86E-02
TI105B-Y3	0.0790	15.2	4.99E-04	7.83E-05	1028	8.08E-02

(a) F-factor at 105 °C = 0.9091; F-factor at 427 °C = 0.8464
(b) F-factor at 105 °C = 0.9128; F-factor at 427 °C = 0.8506

Pacific Northwest National Laboratory

902 Battelle Boulevard
P.O. Box 999
Richland, WA 99354
1-888-375-PNNL (7665)

www.pnnl.gov